

EXPERIMENTAL ANALYSIS OF THE FLOW THROUGH A
BOTTOM OUTLET ON THE THRESHOLD OF MOTION OF
PARTICLES

A THESIS SUBMITTED TO
THE GRADUATE SCHOOL OF NATURAL AND APPLIED SCIENCES
OF
MIDDLE EAST TECHNICAL UNIVERSITY

BY

ÖZGE GÖBELEZ

IN PARTIAL FULFILLMENT OF THE REQUIREMENTS
FOR
THE DEGREE OF MASTER OF SCIENCE
IN
CIVIL ENGINEERING

MAY 2008

Approval of the Thesis;

EXPERIMENTAL ANALYSIS OF THE FLOW THROUGH A BOTTOM
OUTLET ON THE THRESHOLD OF MOTION OF PARTICLES

Submitted by **ÖZGE GÖBELEZ** in partial fulfillment of the requirements
for the degree of **Master of Science in Civil Engineering, Middle East
Technical University** by,

Prof. Dr. Canan Özgen
Dean, Graduate School of **Natural and Applied Sciences** _____

Prof. Dr. Güney Özcebe
Head of Department, **Dept. of Civil Engineering** _____

Asst. Prof. Dr. Şahnaz Tiğrek
Supervisor, **Dept. of Civil Engineering, METU** _____

Prof. Dr. Metin Ger
Co-Supervisor, **Dept. of Civil Engineering, METU** _____

Examining Committee Members:

Prof. Dr. Halil Önder (*)
Civil Engineering Dept., METU _____

Asst. Prof. Dr. Şahnaz Tiğrek (**)
Civil Engineering Dept., METU _____

Prof. Dr. Metin Ger
Civil Engineering Dept., METU _____

Prof. Dr. Melih Yanmaz
Civil Engineering Dept., METU _____

Dr. Hande Akçakoca
GAP Administration _____

Date: 30.05.2008

(*) Head of Examining Committee

(**) Supervisor

I hereby declare that all information in this document has been obtained and presented in accordance with academic rules and ethical conduct. I also declare that, as required by these rules and conduct, I have fully cited and referenced all material and results that are not original to this work.

Name, Last name : Özge Göbelez

Signature :

ABSTRACT

EXPERIMENTAL ANALYSIS OF THE FLOW THROUGH A BOTTOM OUTLET ON THE THRESHOLD OF MOTION OF PARTICLES

GÖBELEZ, Özge

M.S., Department of Civil Engineering

Supervisor: Assoc. Prof. Dr. Şahnaz TİĞREK

Co-supervisor : Prof. Dr. Metin GER

May 2008, 58 pages

The Shield's Diagram has been the key stone for the description of initial motion of a particle in open channel flow. Data in Shield's study and further studies are collected in channels. However, the approximation of these data for the case of withdrawal of sediment or clean water through bottom outlets has not been confirmed. Furthermore, two phase models run to simulate the phenomenon so far have used brine and water combination. In this study, an experimental attempt is made to study the behavior of deposits subject to withdrawal from a bottom outlet where there are not enough parameters to calculate the bottom shear stress and consequently the dimensionless parameters generally used for the description of initiation of motion.

The experimental set up used for this purpose is a 1 m long and 0.35 m wide channel such that at the downstream of the channel there is a horizontal slit representing the bottom outlet. During the experiments, fresh water and sand with $D_{50} = 0.298$ mm and $D_{50} = 0.912$ mm are used. Two different widths of the slit, namely 0.35 m and 0.0875 m are investigated. Based on the observations of the incipient motion of the sediment, the findings in the form of a relationship among the discharge through the bottom outlet, and some other relevant parameters are reported. In addition, a comparison of these data with the literature by the help of some newly defined dimensionless parameters for the description of the initiation of motion is included.

Keywords: Initiation of motion, bottom outlet, Shields diagram

ÖZ

DİP SAVAK AKIMININ KUM DANESİNİN HAREKETE BAŞLAMA EŞİĞİNE ETKİSİNİN DENEYSEL ANALİZİ

GÖBELEZ, Özge

Yüksek Lisans, İnşaat Mühendisliği Bölümü

Tez Yöneticisi : Yard. Doç. Dr. Şahnaz TİĞREK

Yardımcı Tez Yöneticisi : Prof. Dr. Metin GER

Mayıs 2008, 58 sayfa

Shields eğrisi açık kanal akımlarında kum danesinin harekete başlamasının anlatımında büyük önem taşır. Shields'ın çalışmasında kullanılan veriler açık kanal deneyleriyle toplanmıştır. Ancak, bu verilerin katı madde danelerinin veya temiz suyun dip savak yardımıyla çekilmesi için yeterli bir yaklaşım olup olmadığı henüz onaylanmamıştır. Çift fazlı akımı modellemek için şimdiye kadar tuzlu su ve temiz su ikilisi kullanılmıştır. Bu çalışmada, dip savağın birikmiş katı madde üzerindeki etkisi için bir çalışma yapılmıştır. Deney düzeneği 1 m uzunluğunda, 0.35 m genişliğinde, mansapta yatay bir açıklığı bulunan bir kanaldır. Bu açıklığın genişliği ve yüksekliği değiştirilebilmektedir. Deneyler sırasında temiz suyla beraber $D_{50} = 0.298$ mm ve $D_{50} = 0.912$ mm çaplarında iki çeşit kum örneği kullanılmıştır. İlk deney grubunda açıklık genişliği 0.35 m, ikinci deney grubunda ise 0.0875 m alınmıştır. Açıklık

yüksekliđi her iki grupta da 0.0022 m'dir. Gözlemler sonucu katı madde danesinin harekete başlaması eđiđi için elde edilen veriler, açıklıktan geçen debi, açıklık boyutları, kum danesinin çapı arasında bir bađıntıyla ifade edilmiştir. Deneylele elde edilen verilerin Shields'in kullandıđı birimsiz parametrelerle karşılaştırılabilmesi için bu parametrelere açık kanal kanal esasları doğrultusunda bir çevrim metodu da geliştirilmiştir.

Anahtar kelimeler: Tabanda hareket başlangıcı, Dip savak, Shields eğrisi

ACKNOWLEDGEMENT

“Was ihn nicht umbringt, macht ihn starker.”

Friedrich Wilhelm Nietzsche

This study is particularly helpful to clearly define my interests and my future career. It is a pleasure to thank the many people who made this thesis possible.

Special thanks to my supervisor, Dr. ahnaz Tięrek, who gave me opportunities to change the direction of my life more than once. It is difficult to overstate my gratitude to my co-supervisor, Prof. Dr. Metin Ger; this work would not have been possible without the support and the encouragement of him.

I would like to thank Prof. Dr. Melih Yanmaz for his valuable contributions to the study.

Special thanks to Assist. Prof. Dr. Ahmet Cevdet Yalıner for the supply of the sand sample of the Kızılırmak River and to Kıvan Group, Bedri Koza, for the second sample of sand coming from Edirne just with the aim of “a support for an academic study”.

Many thanks for the sincere help of the technicians of Hydromechanics Laboratory; Turgut Ural, Cengiz Tufaner, Hseyin Gndoędu and Mehmet Gkmen. Also Cuma Yıldırım from Materials of Construction Laboratory, Necdet Aydoęan from the department and the Central Laboratory of METU.

Very special thanks go to my family, for giving support in every way of life, especially my sister, Başak Göbelez Cansever, for never ever deducting her belief in me, her backup and support whatever my decision is.

Any words could not be enough in expressing my gratefulness to Erdem Altınbilek for his invaluable support. Very special thanks to Bilge Küçükdoğan, Burak Yılmaz, and Onur Dünder for never leaving me alone. My friends, Iğın Sevin Özdemir, Kemal Arman Domaniç, Özge Küreksiz, Onur Arı were always ready for support in good and bad times.

Finally, and most importantly, I am profoundly grateful to Mustafa Kemal Atatürk. I owe him my being able to write this MS dissertation as a woman while other women in the other parts of the world still fight for their gender rights.

TABLE OF CONTENTS

ABSTRACT	iv
ÖZ	vi
ACKNOWLEDGEMENT	vii
TABLE OF CONTENTS	x
LIST OF FIGURES	xii
LIST OF TABLES	xiv
CHAPTER	
1. INTRODUCTION	1
1.1 Introduction and Literature Review	1
1.2 Scope of the Study.....	2
2. THEORETICAL CONSIDERATION ON INITIATION OF MOTION	4
2.1 General Characteristics	4
2.2 Dimensional Analysis	5
2.3 Analytical Formulation of Shields' Study	10
3. EXPERIMENTAL STUDY	16
3.1 Description of the Experimental Set-up.....	16
3.2 Measurements and Experimental Procedure	25
4. DISCUSSION OF RESULTS	38
4.1 General	38
4.2 Redefinition of Band of Threshold of Motion	38
4.3 Results from Experimental Data	39

4.4 Comparison of Experimental Data with the Conversion of Literature	42
5. CONCLUSION REMARKS AND FURTHER RECOMMENDATIONS	45
REFERENCES	47
APPENDIX	49
A. LABCARD MANAGEMENT AND PROBE CALIBRATION...	49
B. PIV MEASUREMENT	53
C. DATA OF UPPER AND LOWER LIMITS OF SHIELDS DIAGRAM	55
D. A FURTHER RECOMMENDATION ON THE DESCRIPTION OF THE CUMULATIVE INTENSITY CONCEPT	57

LIST OF FIGURES

FIGURES		PAGE
Figure 2.1	Sketch of the system.	7
Figure 2.2	Tractive – force coefficient $\frac{\tau_c}{g(\rho_s - \rho) D}$ against the Reynolds number of the grain $\frac{\rho u_* D}{\mu}$ plotted by Shields.	11
Figure 2.3	Plot of relations derived by Paphitis (2001).	13
Figure 3.1	Top view of the set up (Dimensions are in cm)	18
Figure 3.2	Side view of the set up (Dimensions are in cm).....	19
Figure 3.3	The relationship between the manometer readings difference and discharge.	21
Figure 3.4	Front view of the set up with details. (Dimensions are in mm).....	22
Figure 3.5	Jet flow through the opening with full width (front view)...	22
Figure 3.6	The full width opening right above the flattened sand....	23
Figure 3.7	Grain diameter distribution of two sand samples.	24
Figure 3.8	Sketch of two steps in a set of experiment.	26
Figure 3.9	A visual presentation of the experiment.....	28
Figure 3.10	Visualization of $i < 1$ with respect to the definition based on the location of the particle.	29
Figure 3.11	Visualization of $i = 1$	29
Figure 3.12	Visualization of $i = 2$	30
Figure 3.13	Visualization of $i < 1$ with respect to the definition based on the number of particles removed.....	30

Figure 3.14	Vex versus Cumulative Intensity for each experiment....	36
Figure 4.1	Plot of converted relations, Fr^2 versus Re	39
Figure 4.2	Plot of the experimental data, Fr^2 versus Re	42
Figure 4.3	Comparison of experimental data with Shields diagram.....	44
Figure B.1	Streamlines plotted with the measurement of PIV.....	53
Figure B.2	Velocity vectors plotted with the measurement of PIV....	54
Figure B.3	The velocity profile at $x = 5a$ with a flow of $h \approx 35a$	54
Figure D.1	The relationship between the cumulative intensity and the dimensionless velocity term.....	57

LIST OF TABLES

TABLE		PAGE
Table 2.1	Parameters involved in the dimensional analysis.	8
Table 3.1	Data obtained from the experiments.....	32
Table 4.1	The constant head flow depth and discharge values at cumulative intensity of 3	41
Table 4.2	Average, minimum and maximum values	41
Table C.1	Data of upper and lower limits in details.....	55

CHAPTER 1

INTRODUCTION

1.1 Introduction and Literature Review

Deposition of sediment particles creates major problems in the operation of water resources systems. This is because of reservoirs' essential role in acting as sediment traps, interrupting fluvial sediment transport by producing an almost motionless pool into which flowing solids are deposited. This condition has adverse effects on the initial storage of the reservoir. In addition, reaching of the accumulation to a level of intakes may result in disfunctioning of the intakes. Therefore, different methods for control of sedimentation and rehabilitation of reservoirs, such as dredging, density current venting and flushing, are used. On the other hand, selective withdrawal is also applied in reservoirs, either for sluicing out sediment from the muddy lake or taking in clear water from the upper layer for domestic utilities.

The predictions on deposition of sediment in reservoirs and erosion by the effect of use of an outlet are vital. In this perspective, the information about the initiation of motion is necessary for determining the flow strength at which a given size of sediment will begin to move, and is a necessary input to many sediment transport relations to calculate excess bed shear stress and predict the rate of sediment transport at shear stresses above the critical.

The incipient motion has been studied extensively over the past 60 years, following the work by Shields (1936), who presented a semiempirical approach. Much of the subsequent research into incipient motion builds on the original work of Shields. Paphitis (2002) gives a list of names of several authors, such main ones as White 1970; Mantz 1977; Miller et al. 1977 who have undertaken reviews and extensions of the Shields diagram. On the other hand, only limited comparisons of Shields method against alternative methods for predicting incipient motion have been done. Hjulstrom (1935) and Yang (1973) studied on expressing the phenomenon in terms of velocity related terms rather than shear parameter, as a function of shear Reynolds number. Most of past studies model the phenomenon of initiation of motion in alluvial streams, i.e. flow with velocity profile of logarithmic distribution law.

Usage of a bottom outlet in a reservoir creates a flow, which can be modeled by an orifice, unlike open channel flow. Shammaa et al. (2005) studied the variation of the velocity profiles with distance from a sluice gate, also examined the effect of water depth.

1.2 Scope of the Study

In this study, initiation of motion under the effect of a bottom outlet in a reservoir is studied. For modeling removal of sediment deposited in a reservoir, selective withdrawal is generally used. Most of the time, muddy flow is modeled with the use of brine and water, because removal of sediment starts with the silt, which is deposited nearest to the outlets. However, the case studied herein is somewhat different from routine selective withdrawal or incipient motion studies. This effort must be justified; under the circumstances, described shear stress cannot be discussed or evaluated. For comparison, a conversion for

Shields' diagram in the aim of discarding the shear velocity out of the parameters is studied.

In Chapter 1, an introduction to the subject and review of literature are given with the scope of this study. General characteristics, dimensional analysis and an analytical formulation of Shields' diagram are presented in Chapter 2. Chapter 3 gives the explicit details of experimental set up and experimental procedure. In Chapter 4, the results; and in Chapter 5, discussions and recommendations for further studies are presented.

CHAPTER 2

THEORETICAL CONSIDERATION ON INITIATION OF MOTION

2.1 General Characteristics of Incipient Motion

Sediment transportation can take place in any kind of a conveyance system, such as a closed conduit, an open channel, or along shoreline. The phenomenon of sediment transport is considered as a plane stationary bed consisting of loose and cohesionless (mobile) solid particles, and liquid flowing over it. The case modeled in this study is the flow through a bottom outlet of a reservoir, i.e. constant head flow through an opening. In most of previous studies, the cross-sectional area of the conveyance system throughout a given distance is assumed to be constant, and through the same distance, liquid flow and bed are statistically in a steady state. Accordingly, the average values are considered in solving the problem. The case in this study can be summarized as following; as soon as liquid starts flowing through the bottom outlet of reservoir, hydrodynamic forces are exerted upon the solid particles of the bed in the region deposited behind the opening. A further increase in the flow intensity causes an increase on the magnitude of these forces. After a certain period of time, for the aforementioned region of the stationary bed, a condition is eventually reached at which the particles in the movable bed are unable to resist the hydrodynamic forces and, thus, be first dislodged and eventually start to move. The beginning of the motion is not instantaneous for all particles of a given size resting in the top layer. Actually, due to the

nature of turbulence, the event takes place in a random manner meaning that at any given hydraulic condition, some particles move, some do not move. The condition of the “initial movement of the bed” is determined by observations; therefore, its definition is a very subjective one and therefore several observer – dependent definitions of critical conditions have been made. As an example, Kramer (1935) defined the following three intensities of motion near the critical or threshold condition:

1. “Weak movement indicates that a few or several of the smallest sand particles are in motion in isolated spots in small enough quantities so that those moving on 1 cm² of the bed can be counted.
2. Medium movement indicates the condition in which grains of mean diameter are in motion in numbers too large to be countable. Such movement is no longer local in character. It is not yet strong enough to affect bed configuration and does not result in appreciable sediment discharge.
3. General movement indicates the condition in which sand grains up to and including the largest are in motion and movement is occurring in all parts of the bed at all times.”

The critical fluid conditions at which the individual particles on a sediment bed surface begin to be transported are commonly described by the use of the Shields diagram. This diagram is considered to represent incipient transport from flat beds of maximum stability. The data were determined experimentally by extrapolating sediment transport rate curves to zero. With the use of dimensional analysis, Shields presented the results of his work by defining a shear parameter

as a function of particle Reynolds number. This diagram can be used in any case where it is possible to calculate or at least estimate the value of shear stress at which a given size of uniform sediment will begin to move.

As a comparative work to Shields' diagram, Yang (1973) represented his study in a different point of view. Yang (1973) claim that the rate of sediment transport cannot be uniquely determined by shear stress. With this judgment, Yang (1973) questioned whether critical shear stress should be used as the criterion for incipient motion of sediment transport. Depending on this idea, he studied on defining a dimensionless velocity parameter as a function of particle Reynolds number.

On the other hand, Hjulstrom (1935) plotted the value of velocity versus grain diameter in dimensional form for the effect of flowing water on an erodible bed. Nevertheless, apart from limitation of its application only to water depth equal to or greater than 1 m, its form of being dimensional reduces its common usage. Hjulstrom not only studied on the initiation of motion, but also erosion and suspension are included in his plot. The practical use of values given in this diagram is rather difficult for applications because each case examined is unique when they are considered in a dimensional perspective. But it is clearly seen that this diagram gives an apparent idea about relationship between the particle diameter and the velocity of threshold.

All above-mentioned cases were noted to be studied with uniform open channel flow conditions. The velocity distribution in that case is approximately logarithmic; being zero at the bottom of the channel, the velocity, u , increases rapidly towards the free surface; its maximum value is often found slightly below this free surface (Graf and Altınakar

1998). Briefly, logarithmic velocity distribution law is used in the descriptions of above cases.

However, in case of reservoirs, these estimations are relatively difficult due to larger water depths, complexity of geometry, range of scale and unknown bottom conditions. In addition, logarithmic velocity distribution law is not valid. Therefore, a conversion of parameters is tried for this case.

2.2 Dimensional Analysis

Many constraints are known to affect the critical condition of initiation of motion. It is very useful to analyze these constraints with the use of dimensional analysis. Some parameters representing the case are sketched in Figure 2.1. The parameters involved in dimensional analysis are listed in Table 2.1.

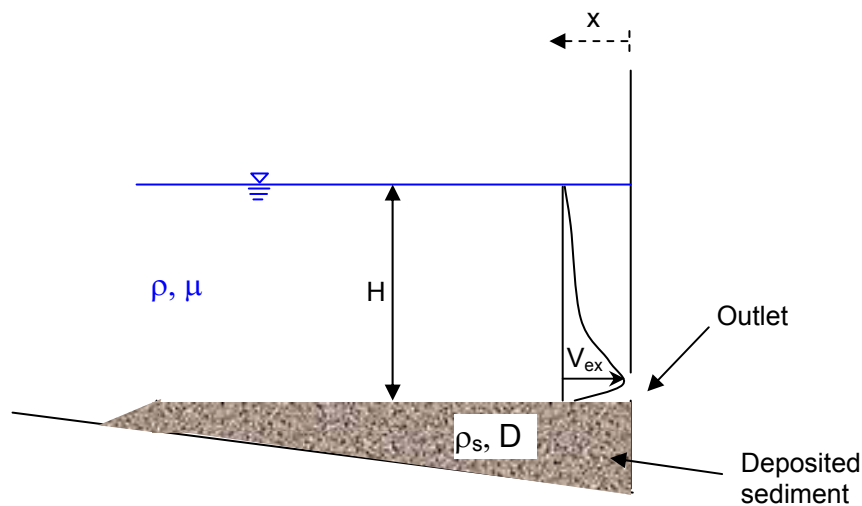


Figure 2.1 Sketch of the system

Table 2.1 Parameters involved in the dimensional analysis

	Symbol	Physical Quantity	Dimension
Flow characteristics	V	velocity of the fluid	[L/T]
	g	gravitational acceleration	[L/T ²]
Properties of fluid	ρ	density of the fluid	[M/L ³]
	μ	dynamic viscosity of the fluid	[M/LT]
Properties of sediment (cohesionless granular material)	ρ _s	density of the sediment	[M/L ³]
	D	median size of the sediment	[L]

Although depicted among the parameters of the system in Figure 2.1, the depth of water, H, is not included in dimensional analysis. In literature, H was included in the velocity term, therefore does not appear directly most of the time. In this study, a direct relationship of H with any other parameter is not studied, therefore H is not listed in Table 2.1.

Functional relationship between the involved parameters can be written as shown in Equation 2.1.

$$f(V, g, \rho, \mu, \rho_s, D) = 0 \quad (2.1)$$

Introducing $\Delta\gamma \equiv g(\rho_s - \rho)$ instead of g, ρ_s and ρ , Equation 2.1 gets the form of Equation 2.2.

$$f(\rho, \mu, \rho_s, D, V, \Delta\gamma) = 0 \quad (2.2)$$

Applying dimensional analysis by taking ρ , D , V as repeating variables, gives the dimensionless terms as Equation 2.3.

$$f\left(\frac{\rho V^2}{\Delta\gamma D}, \frac{\rho_s}{\rho}, \frac{\rho V D}{\mu}\right) = 0 \quad (2.3)$$

In Equation 2.3, the term $\frac{\rho V^2}{\Delta\gamma D}$ is known as the modified grain Froude number and the term $\frac{\rho V D}{\mu}$ is the modified grain Reynolds number. The dimensionless density term, $\frac{\rho_s}{\rho}$, can be included in the further modified version of particle Froude number squared as given in Equation 2.4.

$$Fr^2 = \frac{\rho V^2}{\Delta\gamma D} = \frac{\rho V^2}{g(\rho_s - \rho) D} = \frac{V^2}{g\left(\frac{\rho_s}{\rho} - 1\right) D} \quad (2.4)$$

The relationship between the dimensionless terms is represented as Equation 2.5. The initiation of motion can be described with the use of the modified grain Froude number as a function of the grain Reynolds number.

$$\frac{V^2}{g\left(\frac{\rho_s}{\rho} - 1\right) D} = f\left(\frac{\rho V D}{\mu}\right) \quad (2.5)$$

The tractive force approach lies behind the common use of shear velocity, u_* , for the flow velocity term, V , in order to take both the slope

and flow depth into account implicitly. However, the case studied in this work is not an open channel flow unlike most studies in the literature. The system used in this study is much of like the constant head flow through a slit opening. Therefore, logarithmic velocity assumption turns out to be invalid. So, the exit velocity, V_{ex} , is used as the velocity term throughout the study. At the end, Equation 2.5 gets the form of Equation 2.6.

$$\frac{V_{ex}^2}{g\left(\frac{\rho_s}{\rho} - 1\right) D} = f\left(\frac{\rho V_{ex} D}{\mu}\right) \quad (2.6)$$

Equation (2.6) can be summarized as Equation (2.7).

$$Fr^2 = f(Re) \quad (2.7)$$

2.3 Analytical Formulation of Shields' Study

Shields (1936) have performed several experiments with different ranges of uniformly distributed types of sand. The results of Shields' study were presented as a narrow band with a certain width serving a region below which the traction force is not sufficient to initiate motion, and above which motion is accepted as already initiated. The tractive – force coefficient, θ_* , is plotted as a function of the grain Reynolds number, Re_* , as shown in Equation 2.8 and explicitly in Equation 2.9. The original plot of results of his study is shown in Figure 2.2. The figure is taken from the original translation of Shields' study. The ordinate was named as tractive – force coefficient that is also known as dimensionless shear parameter, or dimensionless shear stress.

$$\theta_* = f(Re_*) \quad (2.8)$$

$$\frac{\tau_c}{g(\rho_s - \rho) D} = f\left(\frac{\rho u \cdot D}{\mu}\right) \quad (2.9)$$

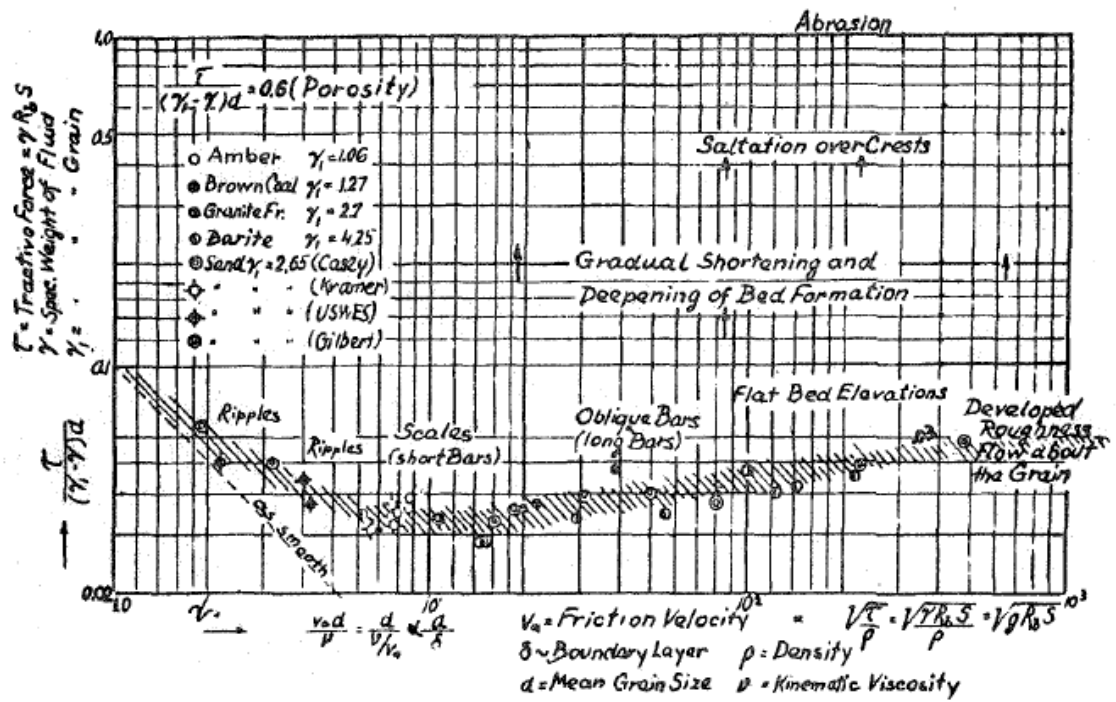


Figure 2.2 Tractive – force coefficient $\frac{\tau_c}{g(\rho_s - \rho) D}$ against the Reynolds

number of the grain $\frac{\rho u \cdot D}{\mu}$ plotted by Shields. (Shields 1936)

There exists numerous researches in literature, which build up additional data points on this diagram. Paphitis (2001) studied the Shields diagram at large including the data added on it from 1914 to 1994 and defined the borders of the broadened band with Equations 2.10 and 2.11.

Lower limit,

$$\theta_{*cr} = \frac{0.075}{0.5 + Re_*} + 0.0300(1 - 0.699e^{-0.015Re_*})$$
$$0.01 < Re_* < 10^5 \quad (2.10)$$

Upper limit,

$$\theta_{*cr} = \frac{0.280}{1.2 + Re_*} + 0.0750(1 - 0.699e^{-0.015Re_*})$$
$$0.01 < Re_* < 10^5 \quad (2.11)$$

The region between the two curves plotted in Figure 2.3 is the band defined by Shields (1936) and broadened by many researchers; e.g. Vanoni (1964), White (1970), Mantz (1977), and others. Shields did not fit a curve to the data but indicated the relationship between the critical dimensionless shear stress and grain Reynolds number with this band. Paphitis (2002) states that the single curve known as the Shields curve was first proposed by Rouse (1939).

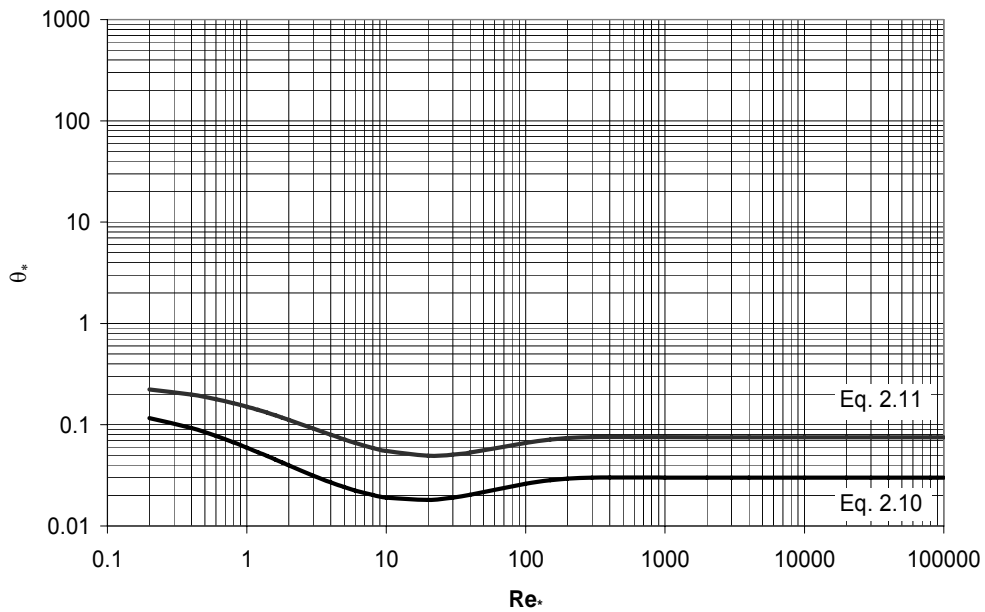


Figure 2.3 Plot of relations derived by Paphitis (2001).

The dimensions of the sediments are relatively small compared to that of the flow parameters; thus, the turbulence will play an essential role in all flows of a mixture consisting of water and sediment. The practical value of those computations lies in the fact that the experimental results are no longer dependent upon model forms (i.e. the experimental channels). Thus, they can be transferred directly to nature.

This study is performed with the aim of giving an idea for the estimation of the critical condition, at which the particles move, in a way of eliminating the shear parameters. In other words, this study enables the estimation of critical condition for the initiation of motion when there is not enough data for the calculation of shear stress and consequently shear velocity. In case of a reservoir, the dimensions make difficulty in calculations which leads us to make new definitions other than Shields' parameters.

As mentioned before, the depth of water and the slope of the channel is involved within the shear velocity. The definition of shear velocity given in Equations 2.12.

$$u_* = \sqrt{\frac{\tau_0}{\rho}} = \sqrt{\frac{\gamma RS_0}{\rho}} = \sqrt{gRS_0} \quad (2.12)$$

In order to discard the shear velocity, and consequently the use of hydraulic radius, R, and slope, S, out of the parameters, the formula made available by Chezy for the uniform flow, Equation 2.13.

$$V = C\sqrt{RS_0} \quad (2.13)$$

where C: the roughness coefficient of Chezy [$L^{1/2}/T$], can be used.

The following procedure is performed on the Shields' parameters defining the initiation of motion. Applying this to the parameters Shields used in Equations 2.14 and 2.16; the conversion coefficients are obtained in Equations 2.15 and 2.17.

$$Re_* = \frac{u_* D}{\nu} = \frac{\sqrt{g}\sqrt{RS_0}D}{\nu} = \frac{\sqrt{g}(V/C)D}{\nu} = \frac{\sqrt{g}}{C} \frac{VD}{\nu} = \frac{\sqrt{g}}{C} Re \quad (2.14)$$

$$Re = \frac{C}{\sqrt{g}} Re_* \quad (2.15)$$

$$\theta_* = \frac{\rho u_*^2}{\gamma_s D} = \frac{\rho g RS_0}{\gamma_s D} = \frac{\rho g (V/C)^2}{\gamma_s D} = \frac{g}{C^2} \frac{\rho V^2}{\gamma_s D} = \frac{g}{C^2} Fr^2 \quad (2.16)$$

$$Fr^2 = \frac{C^2}{g} \theta. \quad (2.17)$$

Many researches have been made on approximation of the value C. It is well known that C depends on the roughness of the pipe and the hydraulic radius and slope of the open channel, i.e. the value of C changes for each single case. Some researchers also studied on fitting a formula for the change of C, but the dimensional form of this constant makes the development and use of a rule much more difficult. Williams and Hazen (1911) presented the results of many experiments of different cases on the value of C. In those tables, the value of C is taken between 40 and 140 in the British unit system. Hec-ras and Heasted Methods (2003) extends this range from 10 to 140. In this study the latest version of this range given by Hec-ras and Heasted Methods (2003) is used. In the SI unit system, the variation of C is given from 5 for very rough surfaces to 77 for very smooth surfaces.

With the help of fittings derived by Paphitis (2001) and the conversions performed with the use of Chezy coefficient, a criterion for the initiation of motion can be defined. This criterion does not require any parameters to calculate or estimate the bottom shear stress.

CHAPTER 3

EXPERIMENTAL STUDY

3.1 Description of the Experimental Set-up

An experimental setup is constructed in the Hydromechanics Laboratory of the Department of Civil Engineering, Middle East Technical University. The system is designed as a closed loop with two reservoirs; one used as a storage at a lower location, the other one as the model (see Figures 3.1 and 3.2).

The model reservoir consists of two adjacent parts. The one with 0.15 m wide and 1.2 m long is the part where the pipe supplying the water is connected. The one next to this has a width of 0.35 m and a length of 1 m. A platform of 0.35 x 0.9 m is attached to the wall of the outlet by a connection that is free to rotate. Another connection is placed at the other end of the platform which enables the change of slope if needed. The sand is laid on the platform up to the level of horizontal slit, simulating an outlet.

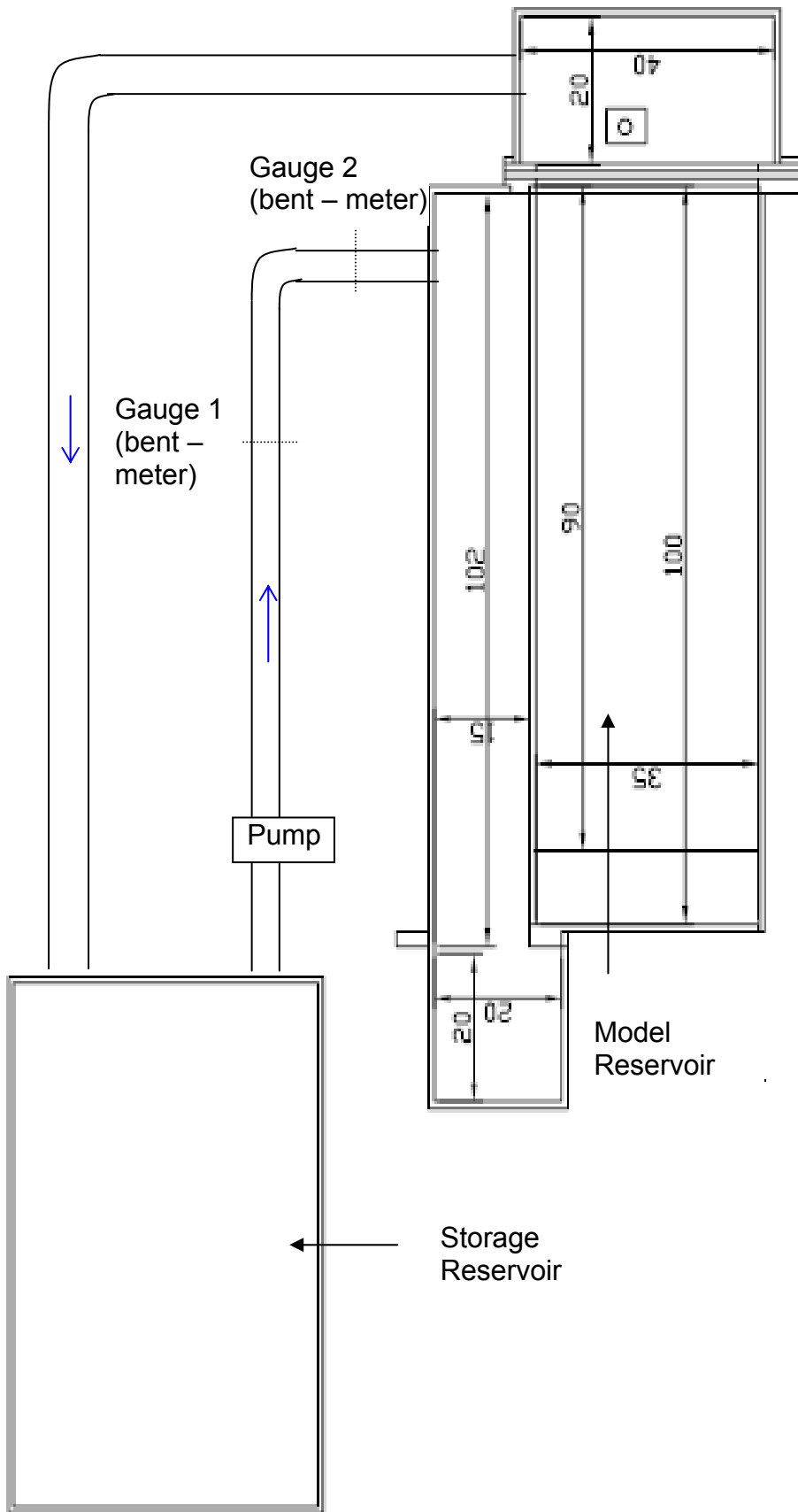


Figure 3.1 Top view of the set up (Dimensions are in cm)

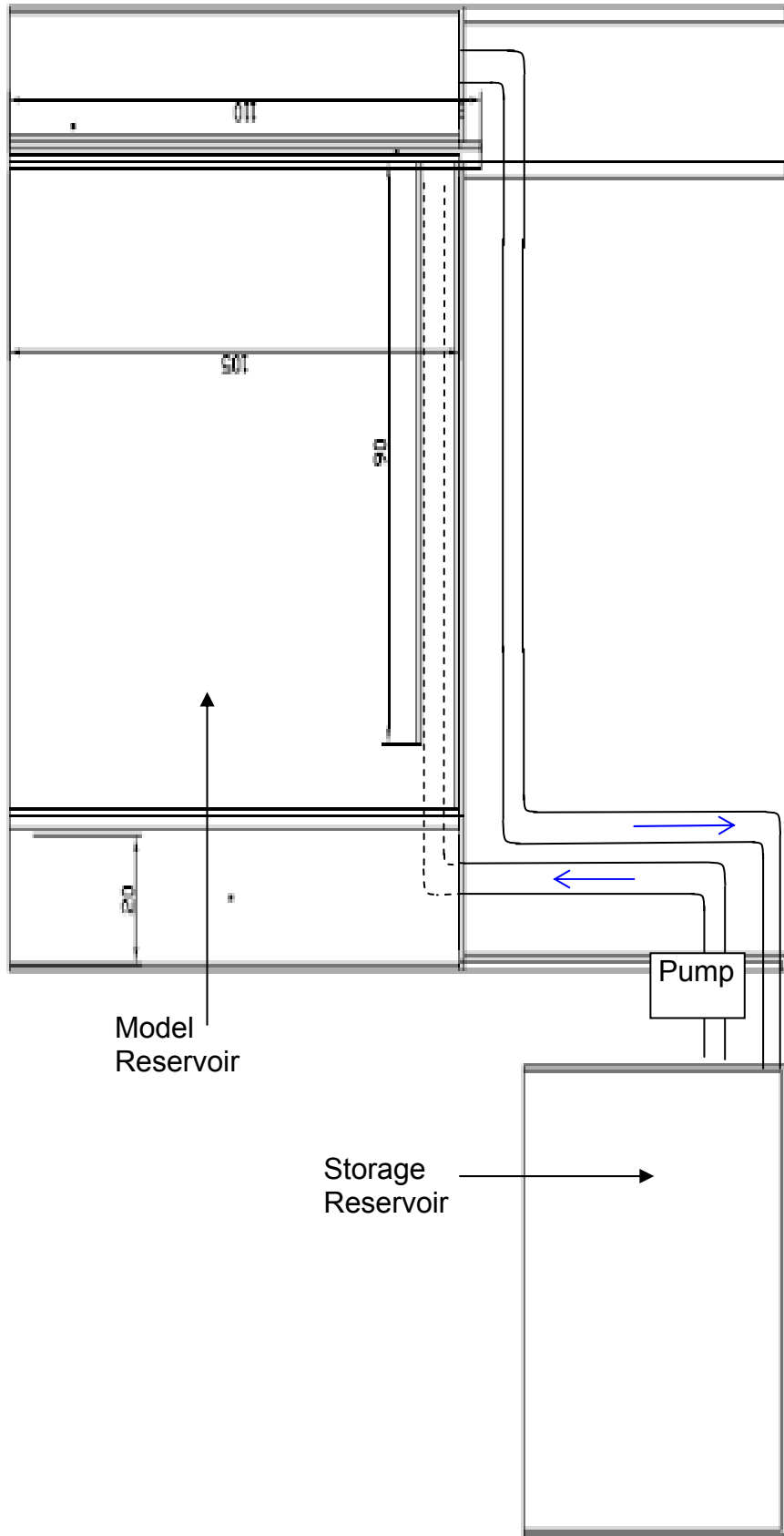


Figure 3.2 Side view of the set up (Dimensions are in cm)

The system is designed to represent a reservoir, therefore the water should flow as if it was released from a large deposit with least disturbances. A horizontal water surface with no waves or disturbances should take place. A direct pipe entrance to the tank cannot provide the case. Hence, the disturbance of water surface is avoided with the use dividing the reservoir into two parts. The pipe is connected to the part which have a width of 0.15 m, and let through a bottom inlet of 1 cm height along the whole length of the wall connecting the two parts.

The discharge is controlled by a butterfly valve located on the pipe which carries water pumped from the storage reservoir up to the model reservoir. The pump has a maximum capacity of 1.5 lt/s with 3 different specific speed levels.

The discharge is measured from a bent – meter with the help of two manometers located on each side of the bent of the pipe carrying water from the storage reservoir to the model one. The location of bent – meter is shown in Figure 3.1.

The calibration of the bent-meter is made by relating volumetrically measured discharges and the corresponding head difference between two locations upstream and downstream of the bend shown in Figure 3.3. The discharge – head difference relation thus obtained is depicted in Figure 3.3. The data are fitted a curve to represent the relationship between the head difference, Δh , and the discharge, Q , passing through the pipe. Equation 3.1 represents the functional relationship such that:

$$Q = 0.0021(\Delta h)^{0.5293} \quad (3.1)$$

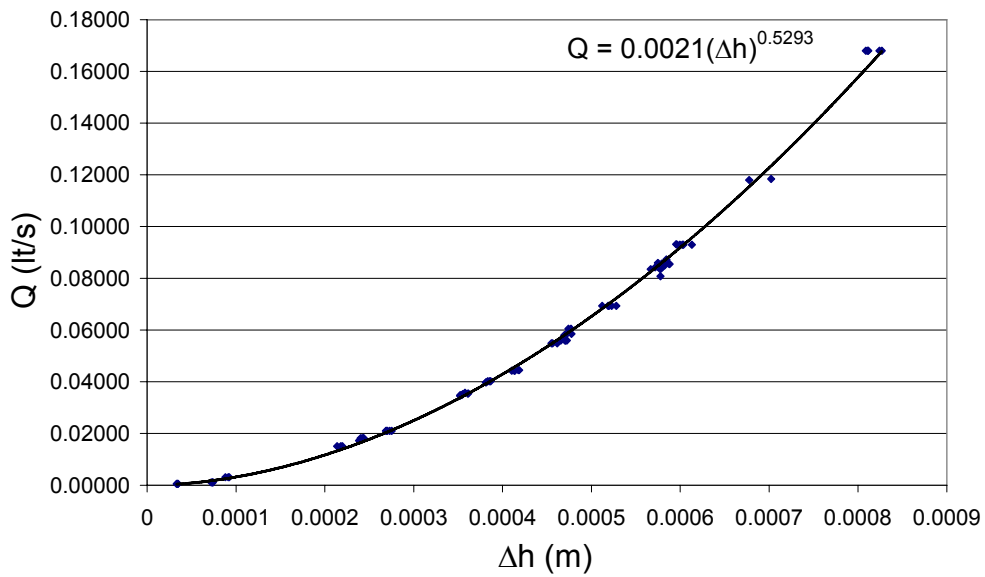


Figure 3.3 The relationship between the manometer readings difference and discharge.

The outlet openings, in the form of horizontal slits, are located on the front face of the reservoir tank. There are 15 slits with the opening height, a , of 2.2 mm along the whole width located at different heights. The first 10 slits are located with 2 cm distance among them above the level of connection of the platform, and the remaining 5 are located with 5 cm distance among them (see Figure 3.4). In this study, only the second slit from the bottom, which is located at 4 cm above the level of connection of the platform, is used (see Figures 3.5 and 3.6 for illustration). For the first set of experiments, the full extent of the slit was used. In later a series of experiments, only quarter of the slit was left open at the center to enhance focusing on the initiation of motion.

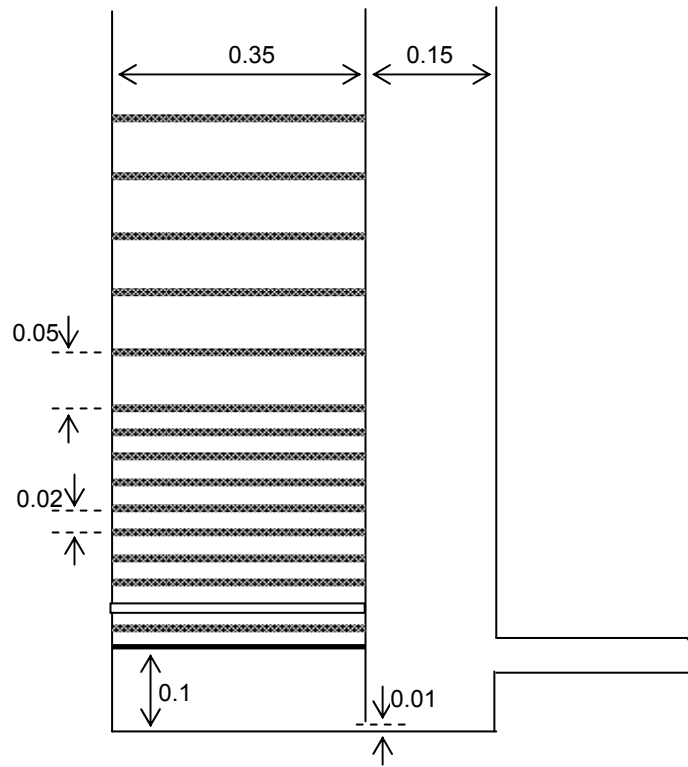


Figure 3.4 Front view of the set up with details. (Dimensions are in mm)

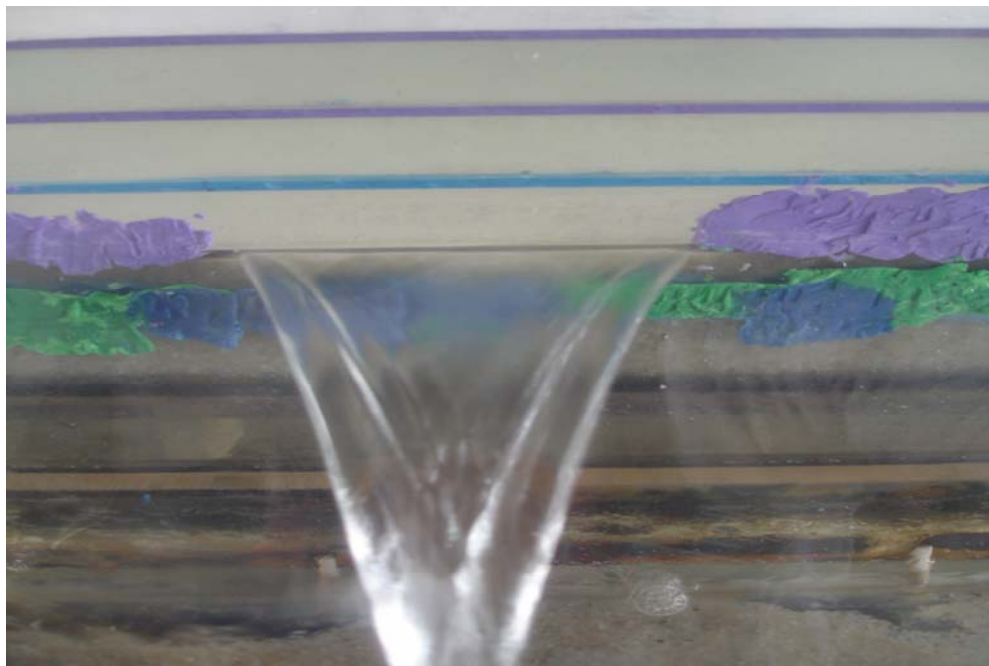


Figure 3.5 Jet flow through the opening with full width (front view).



Figure 3.6 The full width opening right above the flattened sand.

The depth of water is measured by two wave probes which are calibrated with the help of a point gauge in each set of experiment. The usage and calibration procedure of wave probes are given in Appendix A. Data of water surface level taken by the equipment of wave probe are directed to a computer. This helps the observer to decide on the stability of level of the water surface.

Two different types of sands were used. Both sands are quartz sand. $D_{50} = 298 \mu\text{m}$ sample is the sand taken from the Kızılırmak River. The actual distribution of the sand was, $140 \mu\text{m} \leq D \leq 630 \mu\text{m}$. In order to have a more uniform distribution, sieved with two sieves of mesh opening of $210 \mu\text{m}$ and $410 \mu\text{m}$. The second sample with $D_{50} = 921 \mu\text{m}$ is from Edirne. The distribution of this sample is $800 \mu\text{m} \leq D \leq 1190 \mu\text{m}$.

Due to the uniformity of its own distribution, any intervention with sieve is not found necessary. The distribution of the first sample is done with Particle Size Analyzer; the second one with sieve analysis which are performed by Central Laboratory at METU and Materials of Construction Laboratory respectively are plotted in Figure 3.7.

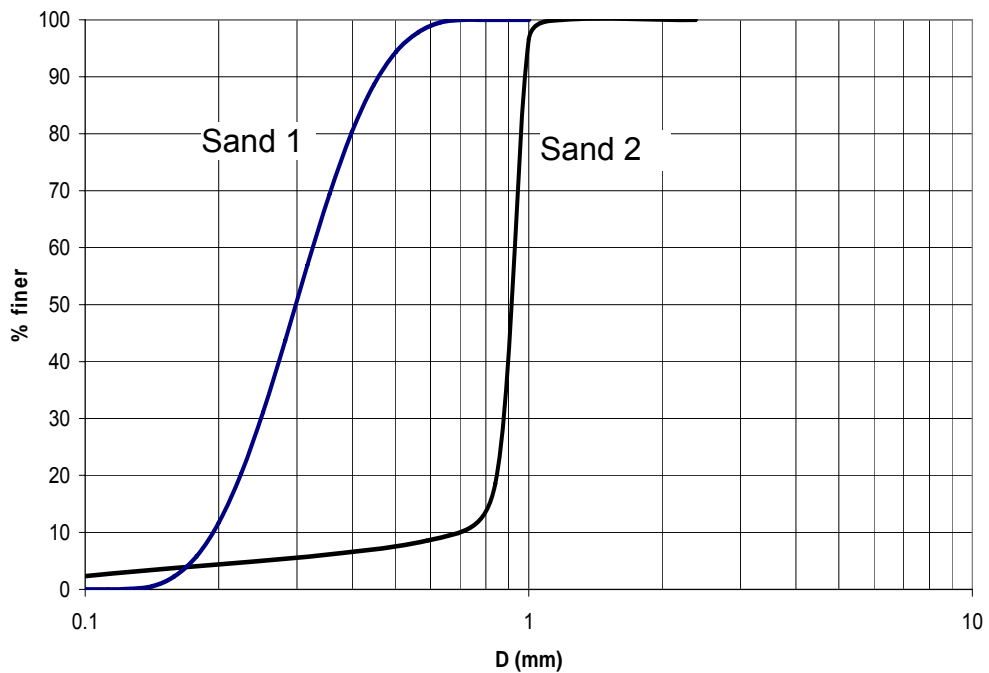


Figure 3.7 Grain diameter distribution of samples Sand 1 and Sand 2.

The uniformity of sand samples can be discussed with the use of the coefficient of uniformity, C_u , of which the definition is given in Equation 3.2.

$$C_u = \frac{D_{60}}{D_{10}} \quad (3.2)$$

If $C_u < 3$, the size distribution of the sand is considered to be uniform. For $D_{50} = 298 \mu\text{m}$ and $D_{50} = 921 \mu\text{m}$, $C_u = 1.682$ and $C_u = 1.236$, respectively. Both sands have a coefficient of uniformity less than 3, meaning that both can be considered as uniform.

3.2 Measurements and Experimental Procedure

Summarizing the previous part, the working principle of the set up is simple. Water is pumped from the storage reservoir to the model. Discharge is controlled with the help of a butterfly valve. Once the water level passes the level of the opening, it starts to spill through the opening. After a certain time, the water level gets stabilized at a given discharge which is set as constant at the beginning of each step by the use of a butterfly valve. At this stage, water level is measured by wave probes, which also allows the check whether the rate of change of water level is minimized or not, in the vicinity of the observation area.

A measurement taken by Particle Image Velocimetry (PIV) for a study at Hydromechanics Laboratory in 2007 is given in Appendix B. The velocity profile is clearly seen at $x = 5a$ with a flow of $h \approx 35a$, where a is the opening height of the slit. The distribution of the velocity profile shows that the flow is different from uniform open channel flow; that is the logarithmic law of velocity distribution is not valid for the present case. Shammaa et al. (2005) states that the maximum velocity right above the bed decreases quickly away from the gate. At $x = a$ and $x = 2a$, the maximum velocity, V_{max} , is about 0.5 and $0.3V_{\text{ex}}$ respectively; where V_{ex} is the average velocity calculated by Q/A . Therefore, the mobility of sand was observed within the distance of twice the opening height of the slit, i.e. $x \leq 2a$, in the present study.

First, the water is pumped to the upper reservoir up to the level of the opening. Pumping is stopped in order to level the sand prior to the experiment. The experiment is run after this preparation stage.

The valve is opened to let a small discharge. A certain period of time is waited to achieve an equilibrium state, i.e. the water level gets constant while the discharge carried by the pipe is approximately the same as the discharge let through the outlet. The first discharge is usually given such that a flow depth of approximately $H = 4a$ develops. The first datum of the experiment is taken at about this stage. The water level is measured with two wave probes and the manometer readings are noted at the same time. In this first situation, the discharge is Q , the water level is H and the velocity of water flowing through the outlet is V_{ex} . Then the discharge is increased by ΔQ , causing an increase, ΔV in the velocity of flow through the outlet which can be observed directly by the increase, ΔH , in water depth. These two steps are sketched in Figure 3.8.

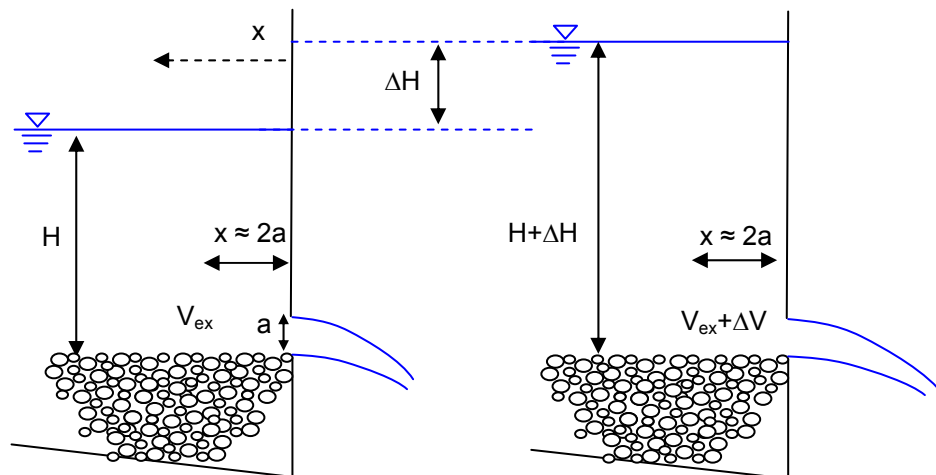


Figure 3.8 Sketch of two steps in a set of experiment.

Between these two steps of the experiments, the observation for the initiation of the motion is made. While, V_{ex} changes by ΔV , the shear stress exerted on the erodible bed increases. A critical stage is reached when some particles are dislodged and flushed throughout the outlet. This means that, unlike open channel flow, saltation is not observed due to the nature of this experiment. The motion of any particle, if there is any, is noted in each step. The notion of intensity of motion and its scale is defined by the author.

An oblique view taken from the observation point is given in Figure 3.9. In this figure, the opening is highlighted with a rectangle. Also the zone of observation is marked with a dashed line. The value of intensity is scaled with respect to the location and/or the number of particles moved in a single step as follows and each value is illustrated with the oblique view zoomed right before the opening:

- i) $i < 1$: A few particles located right near the edge of the outlet are dislodged. The value is noted as 0.5 or 0.75. Figure 3.10 shows an illustration for the location based case.
- ii) $i = 1$: Some particles located approximately at $x = a$ are moved. See Figure 3.11 for the illustration.
- iii) $i = 2$: Some particles located approximately at $x = 2a$ are moved. Figure 3.12 illustrates this case.
- iv) $i \leq 1$: The same values are used in further steps of the experiment. When $i \geq 1$ takes place in a step, and the number of particles moved from the same location as $i \geq 1$ case is decreased, a value of $i \leq 1$ is noted. The illustration of this case is given in Figure 3.13.

- v) $i = 3$: Greater number of particles are transported than the case of $i = 2$.

Mantz (1977) states that, it is first necessary to explain the formal use for describing the beginning of sediment movement as “incipient transport”, rather than “incipient motion.” The writer’s understanding of the latter term is that it describes an instantaneous state, i.e. that for which a solid begins to move. The same idea is included in a cumulative manner in this scaling. When $i > 1$, it is understood that the particles located at $x > a$ move. When a particle located at that distance is dislodged, it sweeps the particles on its way to the outlet with itself. This condition is illustrated with dashed lines placed on both sides of the particle signified in Figure 3.12.

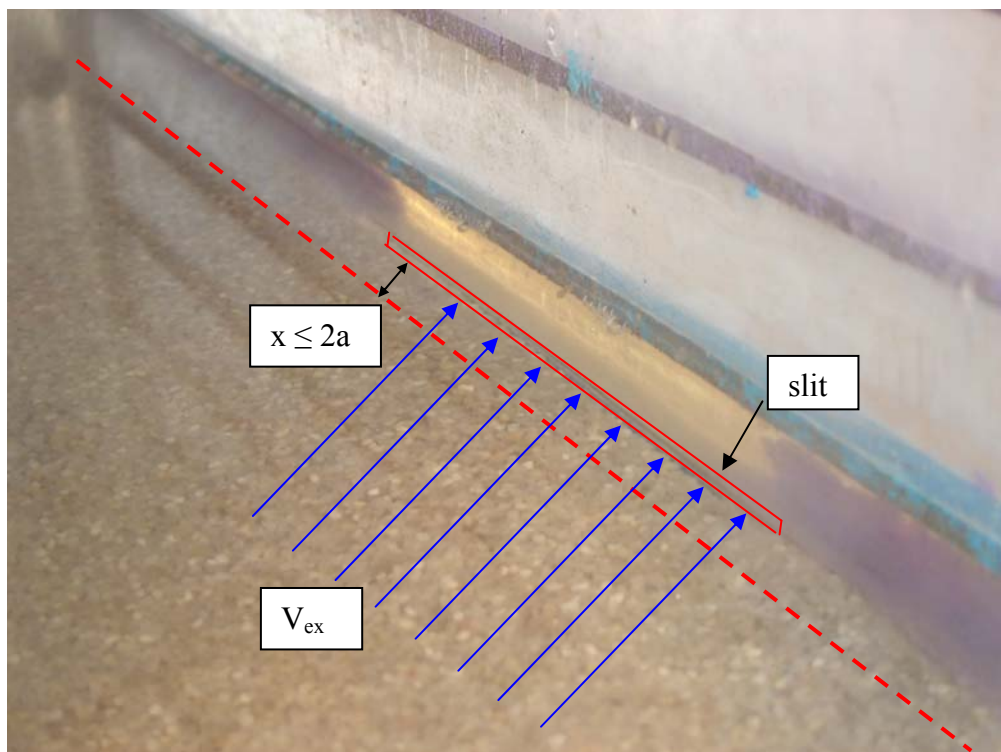


Figure 3.9 A visual presentation of the experiment.

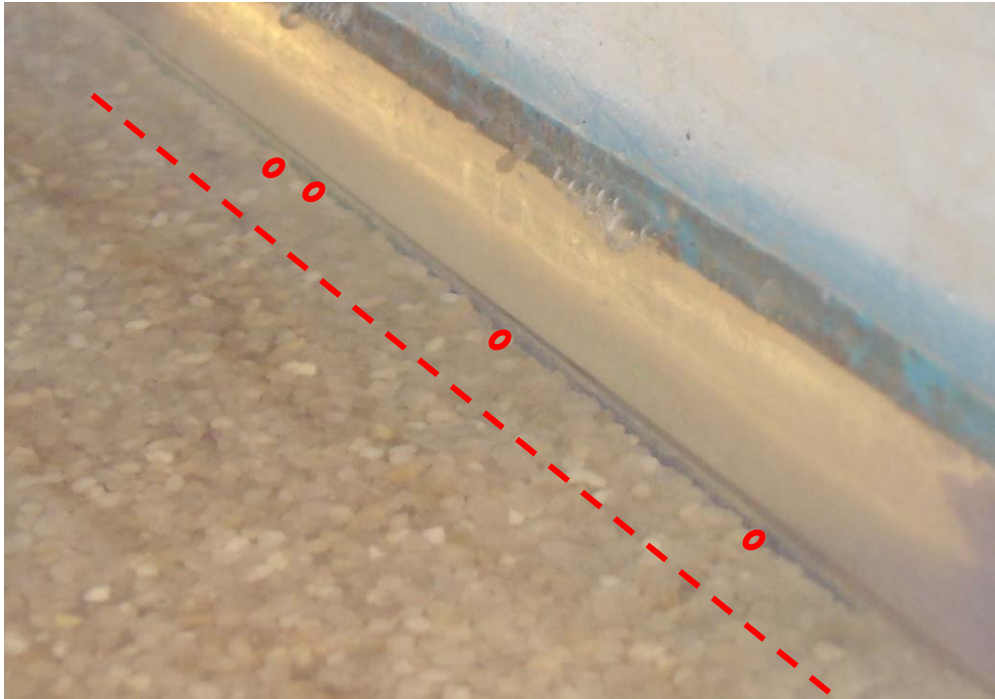


Figure 3.10 Visualization of $i < 1$ with respect to the definition based on the location of the particle.

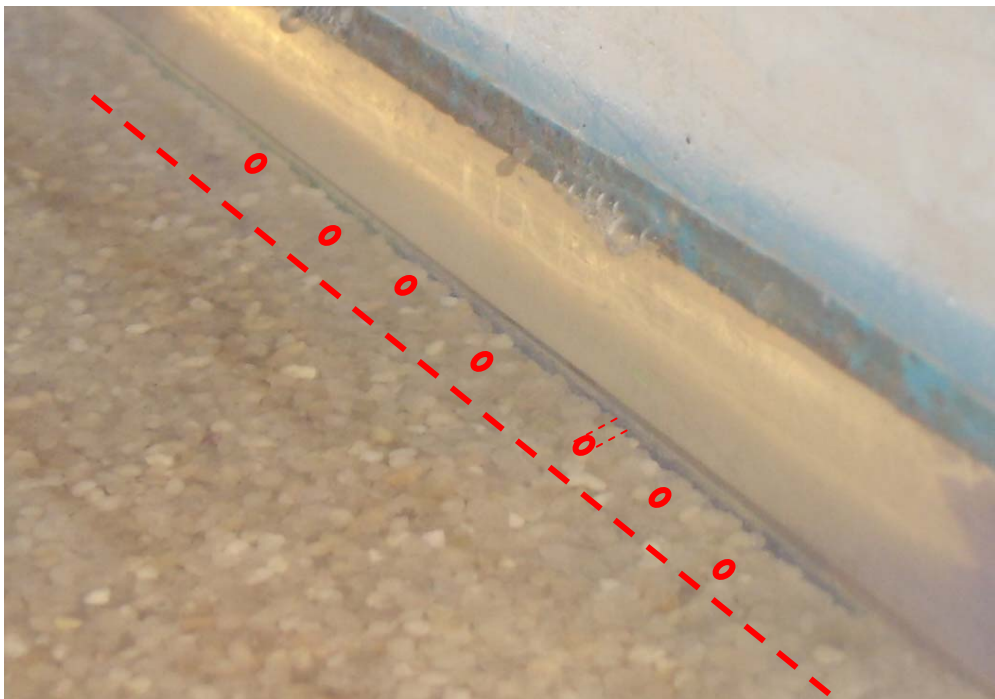


Figure 3.11 Visualization of $i = 1$.



Figure 3.12 Visualization of $i = 2$.

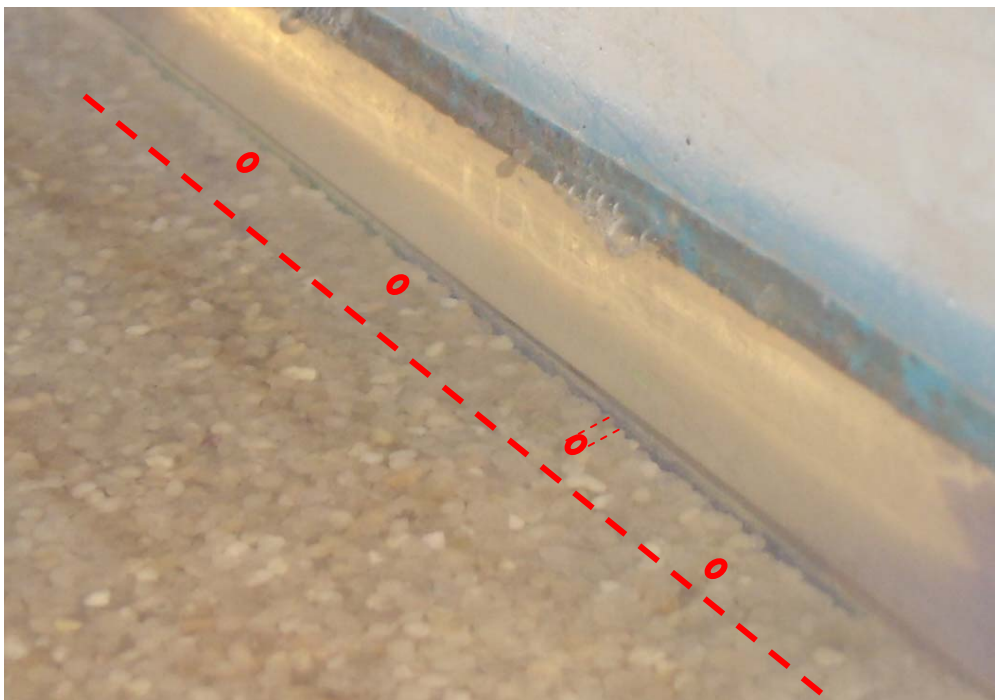


Figure 3.13 Visualization of $i < 1$ with respect to the definition based on the number of particles removed.

The intensity noted in each is step is not used directly for analysis since the set up is designed such that there is no feeding or leveling is made between any steps of the experiment, the intensity values noted are summed up under the heading of cumulative intensity after the experiment. When the cumulative intensity is 3, the incipient transport is accepted to be started.

The value of intensity between each step is directly affected by V_{ex} , that is to say ΔQ . For large ΔQ increment, the increase in shear becomes substantial. In other words, for a very large ΔQ , the intensity value of 3 may be reached in a single step. This is an unwanted situation. The use of cumulative intensity is introduced to have a better identification of incipient transport. With small ΔQ at each step, two values at the beginning and at the end of a single step are not too much apart from each other which gives a better approximation.

The detail of data obtained from the sets of experiments is represented in Table 3.1. In this table, the name of the data set is written in the first column at the level of the first data of the corresponding set. The data number is written in the second column. The third column, designates the constant head flow depth, H , in meters. The column for Δh gives the difference between the two manometer readings for each observation. The entries to Q column are determined using Equation 3.1. i column is the intensity value assigned by the observer, the author of the thesis, based on the observations at each step. Cumulative i , is the cumulative intensity at the end of each step.

Table 3.1 Data obtained from the experiments.

Exp. No	Data	H (m)	Δh (cm)	Q (lt/s)	V (m/s)	i	Cumulative i
3-1	1	0.00608	0.35	0.1053	0.1367	0	0
	2	0.00685	0.43	0.1174	0.1524	0.5	0.5
	3	0.00688	0.71	0.1531	0.1988	0	0.5
	4	0.00728	0.91	0.1746	0.2267	0.5	1
	5	0.00726	1.04	0.1873	0.2433	0.75	1.75
	6	0.00772	1.31	0.2117	0.2749	0.75	2.5
	7	0.00785	1.59	0.2345	0.3046	1	3.5
	8	0.00844	1.68	0.2415	0.3136	1	4.5
3-2	1	0.00640	0.63	0.1437	0.1866	0	0
	2	0.00653	0.89	0.1725	0.2240	0	0
	3	0.00728	1.16	0.1985	0.2578	0.5	0.5
	4	0.00734	1.49	0.2266	0.2943	0.5	1
	5	0.00845	1.73	0.2453	0.3185	1	2
	6	0.00859	1.97	0.2627	0.3412	1	3
	7	0.00986	2.37	0.2897	0.3763	1	4
3-3	1	0.00667	0.283971	0.0942	0.1224		0
	2	0.00712	0.41	0.1145	0.1487		0
	3	0.00748	0.66	0.1473	0.1913		0
	4	0.00770	1.03	0.1864	0.2421		0
	5	0.00805	1.3	0.2108	0.2738	0.5	0.5
	6	0.00805	1.52	0.2290	0.2974	0.5	1
	7	0.00834	1.78	0.2490	0.3234	2	3
	8	0.00912	2.12	0.2731	0.3547	3	6
3-4	1	0.00538	0.51	0.1285	0.1669		0
	2	0.00639	0.77	0.1598	0.2075		0
	3	0.00720	1.09	0.1921	0.2494	0.5	0.5
	4	0.00726	1.39	0.2184	0.2837	0.75	1.25
	5	0.00771	1.66	0.2400	0.3116	0.75	2
	6	0.00840	1.9	0.2577	0.3347	0	2
	7	0.00920	2.18	0.2772	0.3600	1	3
	8	0.00983	2.34	0.2878	0.3737	1	4
	9	0.01059	2.63	0.3061	0.3976	0.25	4.25
3-5	1	0.00505	0.39	0.1115	0.1448		0
	2	0.00576	0.64	0.1449	0.1882		0
	3	0.00671	1.07	0.1902	0.2470		0
	4	0.00756	1.38	0.2176	0.2826		0
	5	0.00871	1.73	0.2453	0.3185	1	1
	6	0.00941	2	0.2648	0.3439	0.75	1.75
	7	0.01027	2.27	0.2832	0.3678	2	3.75

Table 3.1 cont'd Data obtained from the experiments.

Exp. No	Data	H (m)	Δh (cm)	Q (lt/s)	V (m/s)	i	Cumulative i
	8	0.01074	2.47	0.2961	0.3846	0.5	4.25
				0.0000			
3-6	1	0.00701	0.38	0.1100	0.1428		0
	2	0.00754	0.61	0.1413	0.1834		0
	3	0.00743	0.85	0.1684	0.2187		0
	4	0.00769	1.3	0.2108	0.2738		0
	5	0.00848	1.6	0.2353	0.3056	0.5	0.5
	6	0.00930	1.9	0.2577	0.3347	1	1.5
	7	0.01039	2.22	0.2799	0.3635	2.5	4
3-7	1	0.00520	0.56	0.1350	0.1753		0
	2	0.00616	1	0.1835	0.2383		0
	3	0.00690	1.32	0.2125	0.2760		0
	4	0.00809	1.8	0.2505	0.3253	2	2
	5	0.00876	2.02	0.2662	0.3457	1	3
	6	0.00946	2.2	0.2785	0.3617	1.5	4.5
3-8	1	0.00596	0.38	0.1100	0.1428		0
	2	0.00683	0.76	0.1587	0.2061		0
	3	0.00718	1.19	0.2012	0.2613		0
	4	0.00740	1.46	0.2242	0.2912	1.25	1.25
	5	0.00781	1.69	0.2422	0.3146	0.75	2
	6	0.00850	1.94	0.2606	0.3384	2	4
9-1	1	0.01083	0.29	0.0953	0.4950	0	0
	2	0.01314	0.34	0.1037	0.5385	0.5	0.5
	3	0.01411	0.38	0.1100	0.5712	0.5	1
	4	0.01673	0.43	0.1174	0.6098	0.5	1.5
	5	0.02153	0.53	0.1311	0.6812	0.75	2.25
	6	0.02486	0.53	0.1311	0.6812		2.25
	7	0.02735	0.63	0.1437	0.7464	1	3.25
	8	0.03010	0.68	0.1496	0.7772	0.75	4
	9	0.03319	0.74	0.1565	0.8128	0.75	4.75
9-2	1	0.00318	0.2	0.0783	0.4067	0	0
	2	0.00469	0.25	0.0881	0.4576	0	0
	3	0.00598	0.27	0.0918	0.4767	0	0
	4	0.00763	0.3	0.0970	0.5040	0.25	0.25
	5	0.00904	0.35	0.1053	0.5468	0	0.25
	6	0.01083	0.38	0.1100	0.5712	0	0.25
	7	0.01267	0.42	0.1159	0.6022	0.5	0.75
	8	0.01265	0.42	0.1159	0.6022	0.25	1
	9	0.01451	0.44	0.1188	0.6173	0	1
	10	0.01744	0.52	0.1298	0.6743	0.5	1.5

Table 3.1 cont'd Data obtained from the experiments.

Exp. No	Data	H (m)	Δh (cm)	Q (lt/s)	V (m/s)	i	Cumulative i
	11	0.01975	0.59	0.1388	0.7209		1.5
	12	0.02198	0.65	0.1461	0.7589	1	2.5
	13	0.02569	0.74	0.1565	0.8128	2	4.5
9-3	1	0.00723	0.2	0.0783	0.4067	0	0
	2	0.00855	0.23	0.0843	0.4379	0	0
	3	0.01080	0.27	0.0918	0.4767	0	0
	4	0.01154	0.28	0.0935	0.4859	0	0
	5	0.01452	0.29	0.0953	0.4950	0.5	0.5
	6	0.01724	0.34	0.1037	0.5385	0.75	1.25
	7	0.01895	0.38	0.1100	0.5712	1	2.25
	8	0.02060	0.41	0.1145	0.5946	1	3.25
	9	0.02456	0.5	0.1271	0.6605	2.5	5.75
9-4	1	0.00446	0.19	0.0762	0.3958	0	0
	2	0.00647	0.2	0.0783	0.4067	0	0
	3	0.00637	0.2	0.0783	0.4067	0	0
	4	0.00740	0.25	0.0881	0.4576	0	0
	5	0.00897	0.29	0.0953	0.4950	0	0
	6	0.01035	0.31	0.0987	0.5128	0.5	0.5
	7	0.01278	0.36	0.1068	0.5551	0.5	1
	8	0.01281	0.36	0.1068	0.5551	0.75	1.75
	9	0.01497	0.4	0.1130	0.5869	1	2.75
	10	0.01738	0.45	0.1202	0.6246		2.75
	11	0.01923	0.6	0.1400	0.7274	1.5	4.25
9-5	1	0.01332	0.32	0.1004	0.5215	2	2
	2	0.01563	0.38	0.1100	0.5712	1	3
	3	0.01673	0.39	0.1115	0.5791	0.5	3.5
	4	0.01767	0.44	0.1188	0.6173	0	3.5
	5	0.02101	0.48	0.1244	0.6464	0	3.5
	6	0.02308	0.52	0.1298	0.6743	0	3.5
	7	0.02844	0.81	0.1641	0.8526	0	3.5
9-6	1	0.00391	0.22	0.0823	0.4277	0	0
	2	0.00502	0.27	0.0918	0.4767	0	0
	3	0.00502	0.27	0.0918	0.4767	0	0
	4	0.00607	0.29	0.0953	0.4950	0	0
	5	0.00677	0.3	0.0970	0.5040	0	0
	6	0.00771	0.34	0.1037	0.5385	0	0
	7	0.00946	0.38	0.1100	0.5712	0	0
	8	0.01121	0.42	0.1159	0.6022	1	1
	9	0.01320	0.46	0.1217	0.6320	0.5	1.5
	10	0.01546	0.5	0.1271	0.6605	0.75	2.25

Table 3.1 cont'd Data obtained from the experiments.

Exp. No	Data	H (m)	Δh (cm)	Q (lt/s)	V (m/s)	i	Cumulative i
	11	0.01795	0.54	0.1324	0.6879	1	3.25
	12	0.01897	0.54	0.1324	0.6879		3.25
	13	0.02028	0.6	0.1400	0.7274	1	4.25
	14	0.02054	0.6	0.1400	0.7274		4.25
9-7	1	0.00423	0.25	0.0881	0.4576	0	0
	2	0.00613	0.3	0.0970	0.5040	0	0
	3	0.00705	0.35	0.1053	0.5468	0	0
	4	0.00901	0.42	0.1159	0.6022	0.5	0.5
	5	0.01075	0.44	0.1188	0.6173	1	1.5
	6	0.01331	0.49	0.1258	0.6534	0.5	2
	7	0.01546	0.51	0.1285	0.6674	1.25	3.25
	8	0.01844	0.66	0.1473	0.7650	1	4.25
9-8	1	0.00381	0.23	0.0843	0.4379	0	0
	2	0.00455	0.29	0.0953	0.4950	0	0
	3	0.00596	0.32	0.1004	0.5215	0.25	0.25
	4	0.00781	0.36	0.1068	0.5551	0.25	0.5
	5	0.00950	0.44	0.1188	0.6173	0	0.5
	6	0.01148	0.49	0.1258	0.6534	1.5	2
	7	0.01374	0.67	0.1484	0.7711	1	3
	8	0.01590	0.68	0.1496	0.7772	0.5	3.5
	9	0.01893	0.69	0.1508	0.7832		3.5
	10	0.02157	0.75	0.1576	0.8186	1	4.5

Cumulative intensity versus velocity of water passing through the outlet is given in Figures 3.14. Experiment codes starting with numerals 3 and 9 are the ones performed with the sand of $D_{50} = 298 \mu\text{m}$ and $D_{50} = 921 \mu\text{m}$, respectively. As stated in the previous section, discharge is increased with random, yet small steps in each experiment.

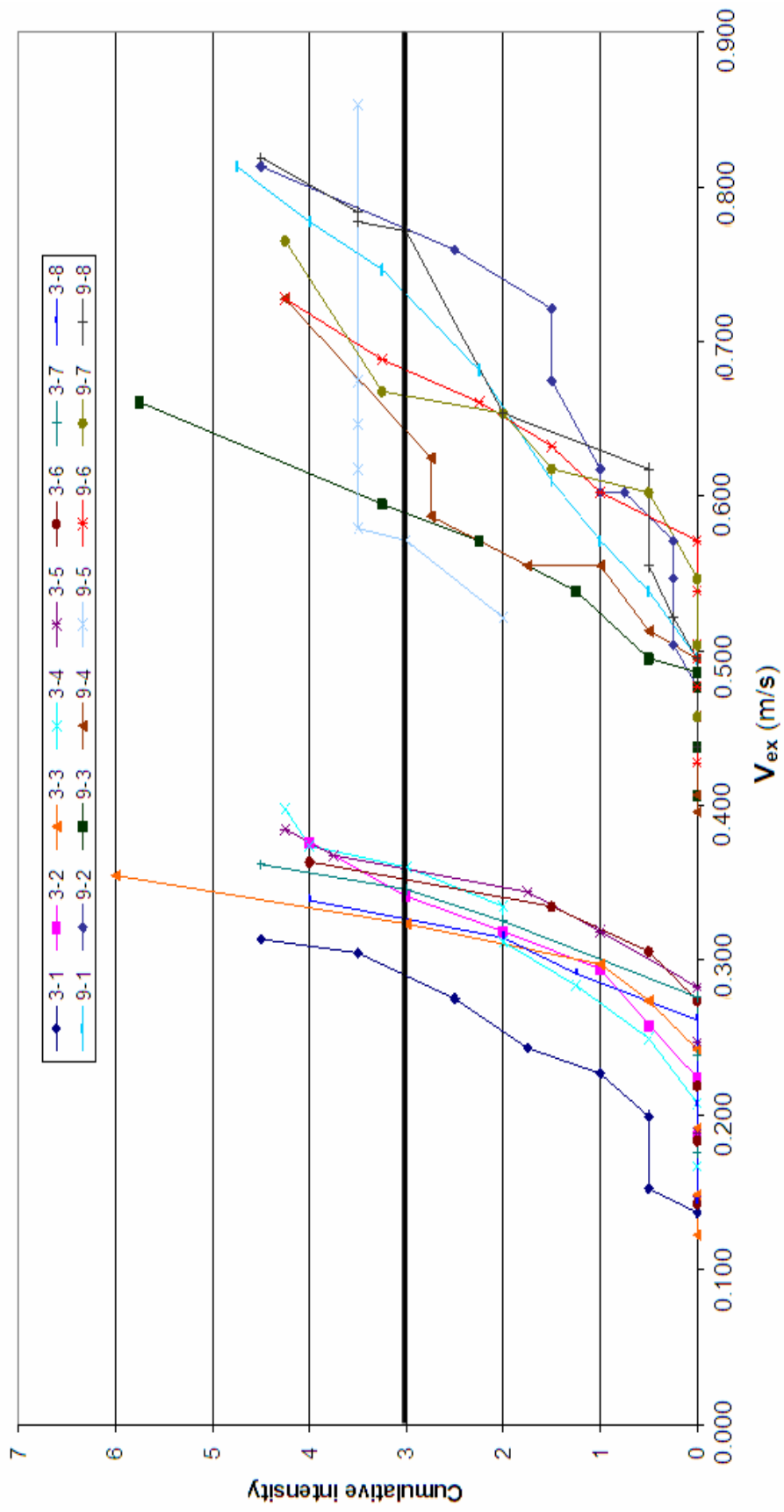


Figure 3.14 V_{ex} versus Cumulative Intensity for each experiment

One can directly see the two distinct group of experiments in Figure 3.14. The group of 3. are in a closer range when compared to the group of 9. set. The reason for this can be the experimental conditions. The ratio of a/D decreases for the second case.

Since the experiment is a rare case, meaning that any similar case could not be found in literature, careful investigations need to be carried out. Rate of change of discharge in each step is very important for precise observation in each step. Water flowing over the bed of sediment exerts forces on the grains that tend to move or entrain them. When discharge is increased with a large step suddenly, the velocity of the flow increases rapidly in that single step. As a result of which, the shear stress exerted by the fluid on the sediment particles increases abruptly. This condition causes a larger number of particles to move in a single step of change of discharge. Since, the velocity corresponding to cumulative intensity of 3 cannot always be exactly achieved, an interpolation procedure is used. Interpolation between small increments in Q gives more precise results than the same procedure performed with larger increments. This situation can be observed in the experiment 9.5 in Figure 3.4.

CHAPTER 4

DISCUSSION OF RESULTS

4.1 Introduction

In this chapter, the results of the experiments are reported with the analysis to compare the findings to newly defined conversion of previous works in literature. The theoretical study on this conversion is given in Chapter 2. In this chapter, a quantitative study is also presented.

4.2 Redefinition of Band of Threshold of Motion

Hec-ras and Heasted Methods (2003) gives the coefficient of Chezy, C , in a range of 5 for very rough surfaces to 77 for very smooth surfaces in the SI system. This study models the flow through an opening in a reservoir. The bottom of the flow may be assumed as a smooth surface because the dimensions of the flow are very large compared to the ones of the particles to be transported. In this wise, the value of Chezy coefficient, C , is considered from the value representing the smoothest case, starting from 77. The upper and lower limits, which belong to the band indicating the initiation of motion, defined by Paphitis (2001) (Equation 2.10 and 2.11) are converted with the value of $C = 77$ with the use of Equations 2.14 and 2.15. Calculations of values for the upper and lower limits of the band are presented in Appendix C.

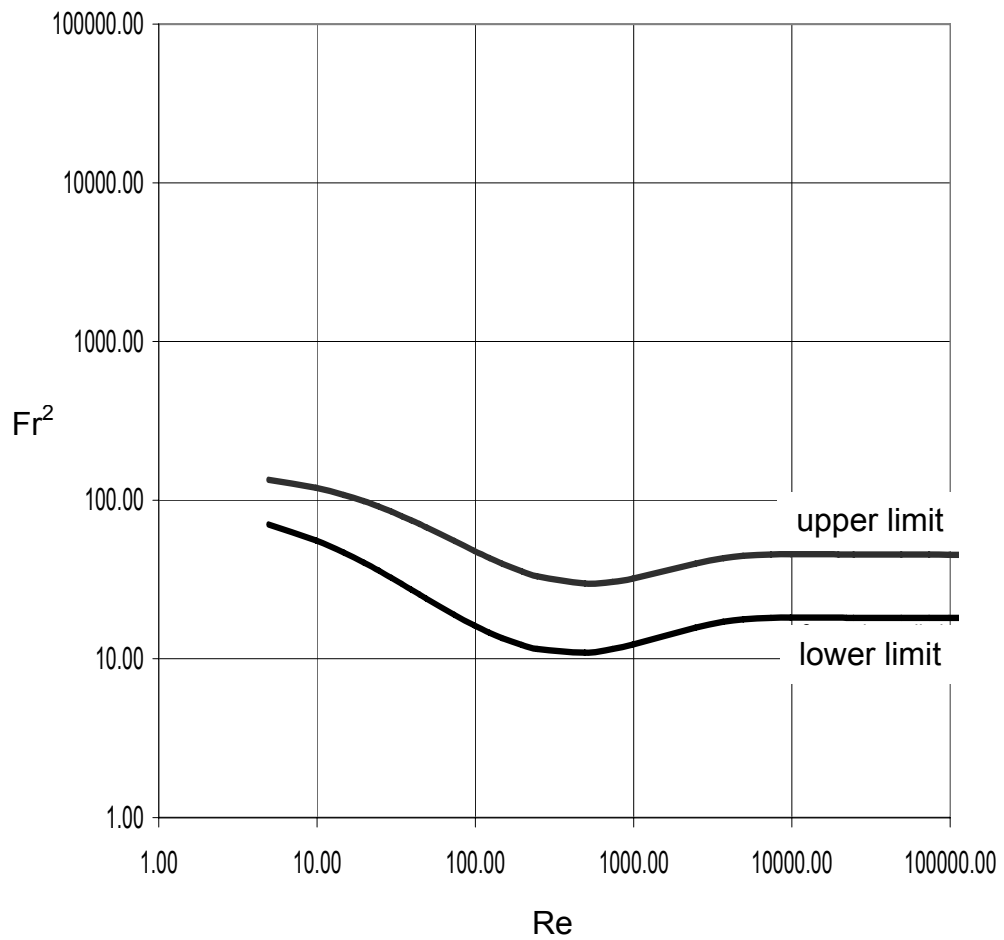


Figure 4.1 Plot of converted relations, Fr^2 versus Re with a value of $C = 77$.

4.3 Results from Experimental Data

The exit velocity, V_{ex} , can either be defined in terms of discharge, Q , or constant head flow depth, H . In this study, V_{ex} is approximated with discharge divided by area of the opening, i.e. $V_{ex} = Q/A$ instead of constant head flow depth relation, $V_{ex} = \sqrt{2gH}$ which is valid for inviscid

flow. When replaced to the general relation given in Equation (2.5), the following relation is obtained.

$$\frac{(Q/A)^2}{g\left(\frac{\rho_s}{\rho} - 1\right) D} = f\left(\frac{\rho(Q/A)D}{\mu}\right) \quad (4.1)$$

Equation (4.1) considers the direct effect of discharge and the dimensions of the outlet on the flow. In fact, these parameters are also the directly controllable variables of the experiment. Hence, the definition of velocity in terms of discharge and area of outlet give rise to further studies related to this subject in a more functional way. The constant head flow depth and discharge values at cumulative intensity of 3 are given in Table 4.1. The plot of Re versus Fr^2 for the two samples are given in Figure 4.2. In calculations, D_{90} values of both samples are used. The reason for the case is that, the particle size distributions of both samples are so uniform that the threshold of the particles 90% finer may represent the whole picture. An example of the use of D_{90} in calculation of a parameter of initiation of motion of a particle can be observed in Yanmaz (2002), which uses the definition of

shear velocity acting on a particle $u_* = \frac{u\sqrt{g}}{18 \log\left(\frac{12 R}{3 D_{90}}\right)}$.

Table 4.1 The discharge values at cumulative intensity of 3

Data No	Q_{meas} (lt/s)	V_{ex} (m/s)	Re	Fr²
3.1	0.223	0.290	133.221	11.265
3.2	0.263	0.342	157.117	15.668
3.3	0.231	0.300	138.000	12.087
3.4	0.249	0.323	148.753	14.045
3.5	0.2754	0.358	164.525	17.180
3.6	0.276	0.358	164.883	17.255
3.7	0.271	0.352	161.896	16.636
3.8	0.266	0.345	158.909	16.028
9.1	0.1405	0.730	715.273	33.582
9.2	0.1485	0.771	756.000	37.516
9.3	0.113	0.587	575.273	21.723
9.4	0.1235	0.642	628.727	25.947
9.5	0.11	0.571	560.000	20.585
9.6	0.131	0.681	666.909	29.195
9.7	0.128	0.665	651.636	27.873
9.8	0.14805	0.769	753.709	37.289

Table 4.2 Average, minimum and maximum values

		V_{ex} (m/s)	Re	Fr²
Set 3.	Average	0.334	153.413	15.021
	Minimum	0.290	133.221	11.265
	Maximum	0.358	164.883	17.255
Set 9.	Average	0.677	663.441	29.214
	Minimum	0.571	560.000	20.585
	Maximum	0.771	756.000	37.516

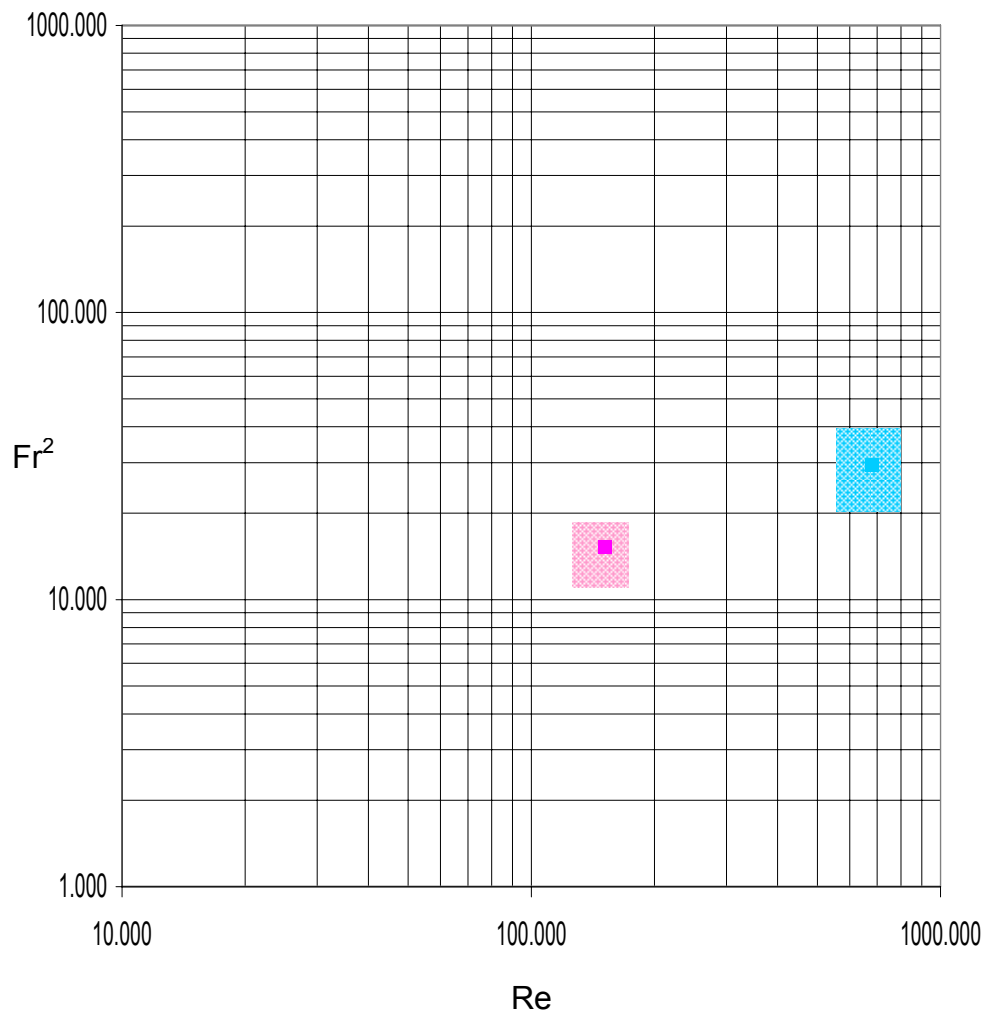


Figure 4.2 Plot of the experimental data, Fr^2 versus Re .

4.4 Comparison of Experimental Data with the Conversion of Literature

Plot of experimental data on the band representing the initiation of with converted dimensionless parameters, Fr versus Re is given in Figure 4.3.

The plot shows that the experimental data stands in the region of the critical region, where the force exerted on the particles is enough to move them. The position of the sample with $D_{50} = 298 \mu\text{m}$, is very well fitted inside the band. However, when the diameter of the sample is increased, the irregularity of the bottom will increase.

The results show that, a conversion of Shields' parameters makes it possible to consider the initiation of motion without considering shear stress as a parameter. This is important for the velocity distributions other than logarithmic profile and including the conditions at which a calculation for the stress is not possible. In case of a reservoir, when the dimensions and the conditions are considered, an estimation of velocity of water released from the bottom outlet may give a better idea than an estimation of bottom shear stress.

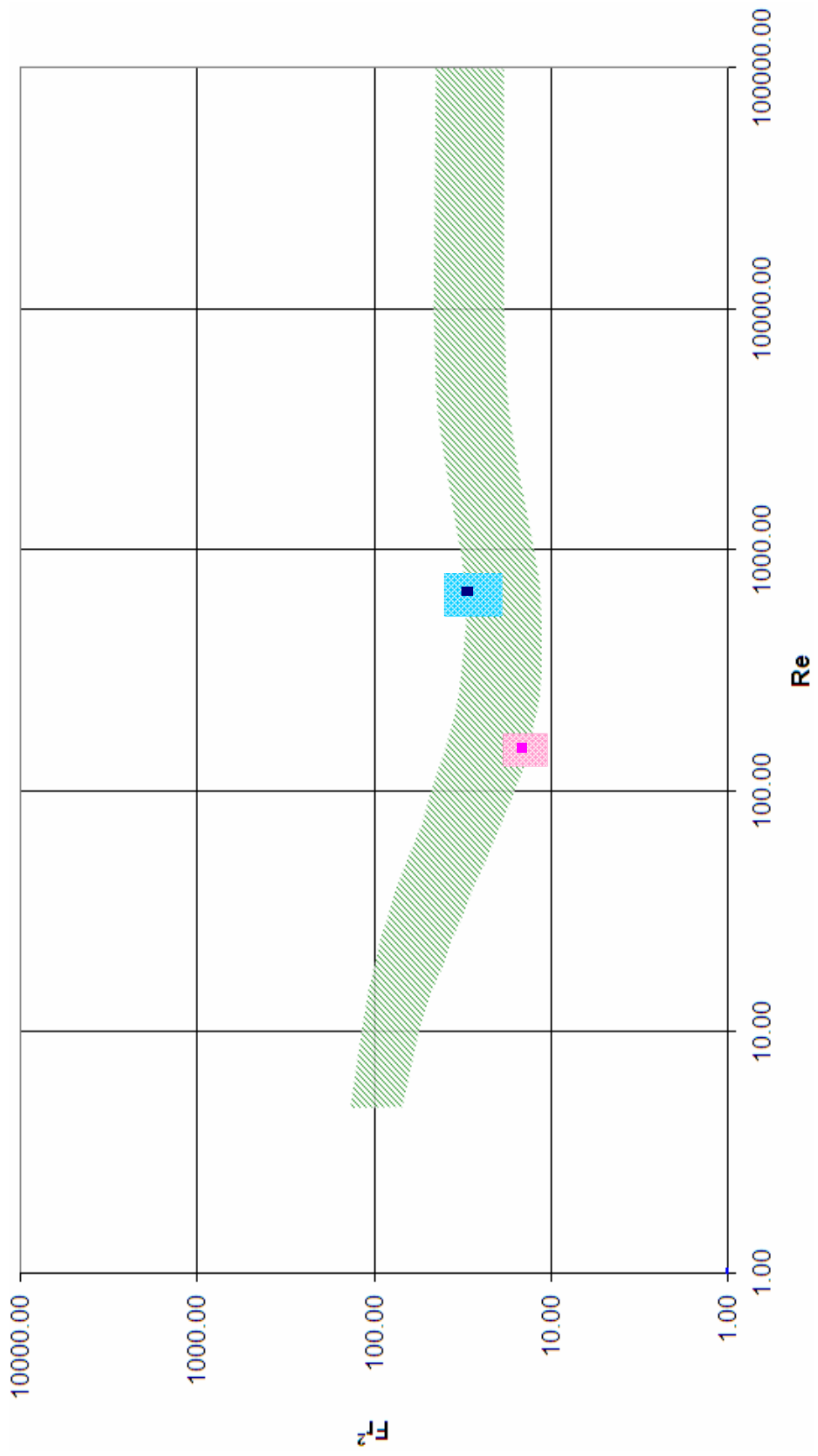


Figure 4.3 Comparison of experimental data with Shields diagram.

CHAPTER 5

CONCLUSION REMARKS AND FURTHER RECOMMENDATIONS

In Chapter 4, it is understood that the use of exit velocity of flow of water through the bottom outlet of a reservoir is acceptable as a criterion for the initiation of motion. A different velocity profile can be compared with the conversion of parameters of Shields. The experimental study proves this claim.

This study may also be compared with the study of Yang's. But the velocity term used in this study is the exit velocity, V_{ex} . This is because the real value of velocity along the plane of the outlet is too much different than the average value of velocity. Yang used the logarithmic law of velocity distribution in representing his study. A conversion between two different velocity profiles is not studied. Conversion of shear parameter seems better and easier to express the results.

While studying on an experimental case such as the present one, the observer requires a good definition for the initiation of motion of particles. The author's intensity scale is defined for this purpose. The motion once started continues in further steps because larger discharge values move particles located at a distance larger than the observation area. After a while, a condition takes place which can be named as erosion rather than initiation of motion.

Also, any comparison with selective withdrawal studies has not been made. Hjulstrom's diagram shows that in erosion; very small particles

are moved with velocity of flow as high as velocity needed to move very coarse particles. This is due to cohesive forces, which are inevitable when the particles have very small dimensions.

Many further studies can be build up on this study. The experimental set – up is a very flexible one, therefore sand samples used and the dimensions and location of the slit, the slope of the bottom of the model reservoir may be changed to many alternatives. For example, the bottom outlet on a dam can better be modeled by a circular orifice by including the geometric properties of the orifice in the dimensional analysis.

Because the aim of this study does not include the quantitative measurement of the sediment particles transported, the system is used in a way to enable the observation of the threshold of initiation of motion. Quantitative measurements mentioned as above can be carried out more precisely with optical equipment measuring concentrations, e.g. PIV is a very useful tool for this purpose.

Another further study can be made on defining the cumulative intensity concept given by the author of this study in a more systematic scheme. Because of the limitation of the number of data collected for this study, instead of a generalized method, only a preliminary study for this definition is included in Appendix D. A further study on the definition of this subject would make the use of bottom outlets more feasible because the rehabilitation of reservoirs filled with sediment is very important in near future of hydropower structures.

REFERENCES

Chow, Ven Te, 1919 - *Open-channel hydraulics*, New York: McGraw-Hill, 1959.

Graf and Altınakar, *Fluvial Hydraulics*, London: Wiley, 1998.

Hjulström F., Studies of the Morphological Activity of Rivers as Illustrated by the River Fyris, Bulletin, Geological Institute of Upsala, Vol. XXV, Upsala, Sweden, 1935.

Kramer H., *Sand Mixtures and Sand Movement in Fluvial Models*, Transactions, ASCE, Vol. 100, Paper No. 1909, 1935, pp. 798-878

Mantz P.A., *Incipient transport of fine grains and flakes by fluids-extended shields diagram*. Journal Hydraulic Division, 103, 601– 615, 1977.

Paphitis D., *Sediment movement under unidirectional flows: an assessment of empirical threshold curves*, *Coastal Engineering* 43, 227-45, 2001.

Williams G. S., Hazen A., *Hydraulic tables; the elements of gagings and the friction of water flowing in pipes, aqueducts, sewers, etc. as determined by the Hazen and Williams formula and the flow of water over sharp-edged and irregular weirs, and the quantity discharged, as determined by Bazin's formula and experimental investigations upon large models*, New York : J. Wiley & sons, 1911

White S.J., *Plane bed thresholds of fine grained sediments*, *Nature* 228, 152–153, 1970.

Shammaa Y., Zhu D.Z., Rajaratnam N., *Flow Upstream of Orifices and Sluice Gates*, *Journal of Hydraulic Engineering*, Vol. 131, No. 2, February 1, 2005.

Shields, A. (1936), "Anwendung der Aehnlichkeitsmechanik und der Turbulenzforschung auf die Geschiebebewegung." Mitteilungen der Preussischen Versuchsanstalt für Wasserbau und Schiffbau, Heft 26, Berlin, Germany (in German), (English translation by W. P. Ott and J. C. van Uchelen available as Hydromechanics Lab., California Inst. of Tech., Pasadena).

Şimşek Ç., *Forced Hydraulic Jump on Artificially Roughened Beds*, METU, 2006.

Vanoni V.A., *Sedimentation engineering*, the ASCE Task Committee for the Preparation of the Manual on Sedimentation of the Sedimentation Committee of the Hydraulics Division, New York : The Society, 1964.

Yang, C.T., *Sediment Transport Theory and Practice*, Journal of Hydraulic Engineering, Vol. 98, No. HY10, Proceeding Paper 9295, pp.1805-1826.

Yanmaz M. A., *Köprü Hidroliği*, METU Press, Ankara, 2002.

APPENDIX A

LABCARD MANAGEMENT AND PROBE CALIBRATION

This part is taken originally from Şimşek (2006):

“The following text is taken from the web page <http://www.churchillcontrols.co.uk/downloads/wmman.pdf> in order to set up and use the Labcard in the Hydromechanics Laboratory at METU prior to experimental stage of this study. Since necessary documentation is not accessible in the Laboratory, the following text will certainly be helpful for prospective researchers and Labcard users and in new studies. As a final remark, it should be reminded to new researchers that the software “470.exe” should be run in DOS operating system on the computer in the Hydromechanics Laboratory at METU in order to take the digitalised output of the analog data sent by the Labcard.

There are two settings, one for the frequency and one for sensitivity made on the circuit card. For these the module must be withdrawn from the case.

FREQUENCY SELECTION

The energisation frequency of the probe is selected by inserting a jumper into one of a series of 6 card mounted pins. Each pin is labelled with the approximate frequency. When probe are used in close

proximity to each other there is some advantage in operating the probe at the highest frequency to reduce the ripple content of the output signal.

SENSITIVITY SWITCH

The small jumper mounted in the circuit board alters the amplitude of the energisation voltage which is applied to the SET DATUM control. For probes up to 500 mm in length the jumper should be set to position "S", i.e. with its jumper moved towards the front panel.

For longer probes the jumper should be set to position "L", i.e. towards the rear plug connector to reduce the sensitivity of the SET DATUM control.

CONNECTION OF PROBE

The probe may be connected either to the red 4 mm sockets on the front panel by means of the plugs provided, or by means of terminal connections at the back. The connecting cable should be a twisted pair or a flat "figure 8". No special characteristics are required and a suitable cable would be one consisting of 2 conductors each 7/0.25 mm (2 amp). The energisation voltage is balanced about earth so it is important that neither of the conductors is earthed.

LEAD COMPENSATION

The instrument incorporates means for compensation for the resistance of the connecting cable to ensure that a high degree of linearity of measurements is maintained over a very wide dynamic range of probe

conductivity. Disconnect the probe cable at the probe end and insert the plugs into the blue TEST sockets on the front panel. Depress the toggle switch into the TEST position, turn the SET OUTPUT control to its fully clockwise position, (i.e. maximum) and adjust the SET DATUM control until the pointer of the balance meter is in its central position (rotating the control clockwise raises the meter pointer). Depress the push button and rotate the COMP control with a screwdriver to restore the pointer to its balance position. Correct compensation is achieved when pressing and releasing the push-button results in no change in the position of the meter pointer. The plugs can then be removed from the TEST sockets and reconnected to the probe.

OUTPUT SIGNALS

The instrument provides an output signal with a centre zero at earth potential and with maximum excursions of + and - 10 volts. Connections can be made either to the OUTPUT coaxial plug on the front panel or by terminal connections at the rear where the following signals are available:-

Terminal 1: 10V; 0; -10V

Terminal 2: 10mA; 0; - 10mA from a source impedance of 1 K ohm.

Terminal 3: 0.05 mA; -0.05 mA with a parallel resistance of 240 ohms for galvanometer recorder. (Galvo. SMI/S).

The frequency response of the output signals is limited by the smoothing filter in the rectifier circuit which has a 95% response at 10Hz.

SET DATUM

This enables the output signal to be set to zero, i.e. to earth potential, for any initial depth of probe immersion. The instrument will then give its maximum full scale output of + and - 10 volts for waves which just reach the bottom of the probe in their troughs. To set up the control, fix the probe in position immersed to the required depth in still water, set the toggle switch on the front panel to the OPERATE position, set the SET OUTPUT control to its fully clockwise position, and then rotate the SET DATUM control to bring the indicating meter to its central position.

SET OUTPUT

This control attenuates the output signal and enables it to be set for a maximum voltage of any value between zero and 10 volts. Provided the datum has been adjusted as described in the previous paragraph the dial calibrations read directly in volts and/or milliamps. All that is required is to set the dial to required output and to lock it. Note that in doing so, the sensitivity of the datum adjustment and the cable resistance compensation described above is reduced, and it is recommended that this control always be set to its maximum before carrying out these operations.”

APPENDIX B

PIV MEASUREMENT

The PIV measurement taken for the velocity profile of the constant head flow through the same opening used in this study with a second platform placed right at the level of the lower boundary of the opening. The depth of flow is approximately $35h$. Streamlines and velocity vectors are given in Figure B-1 and B-2 respectively. The velocity profile at $x = 5a$ is shown in Figure B-3.

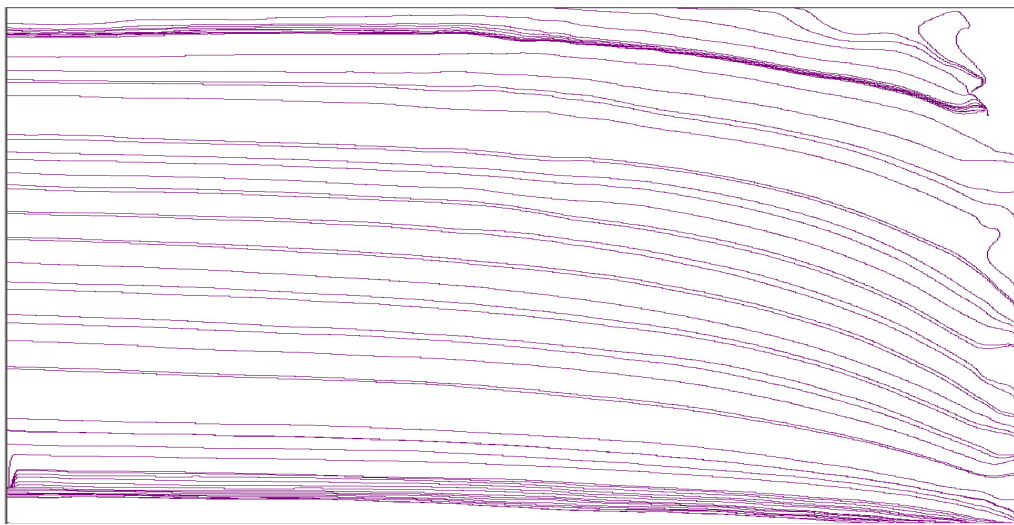


Figure B-1 Streamlines plotted with the measurement of PIV

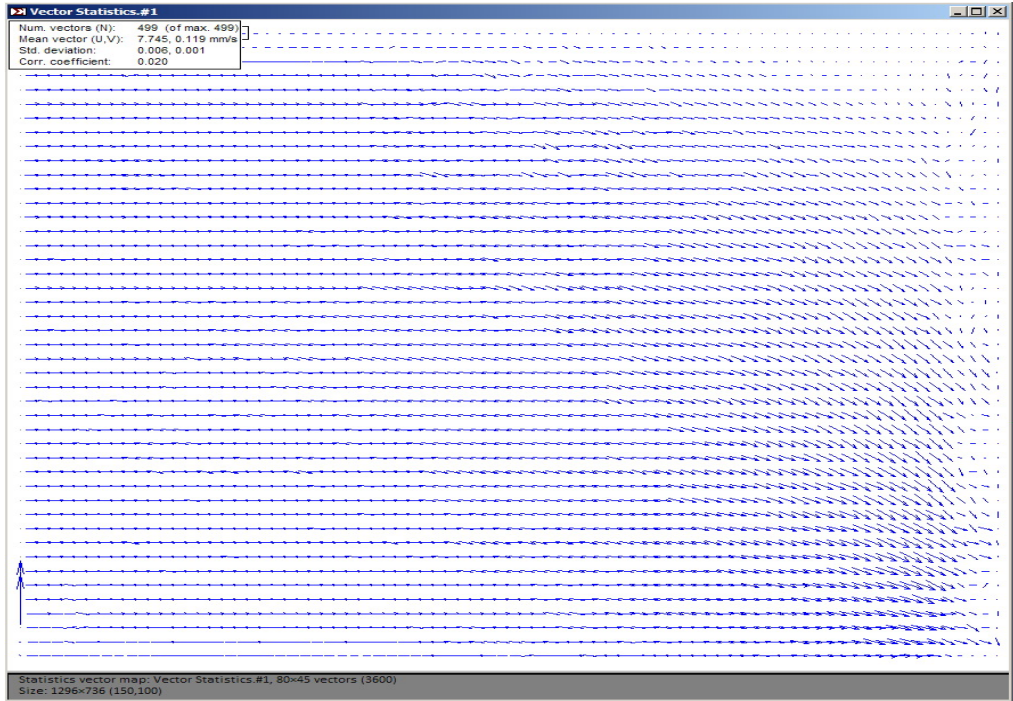


Figure B-2 Velocity vectors plotted with the measurement of PIV

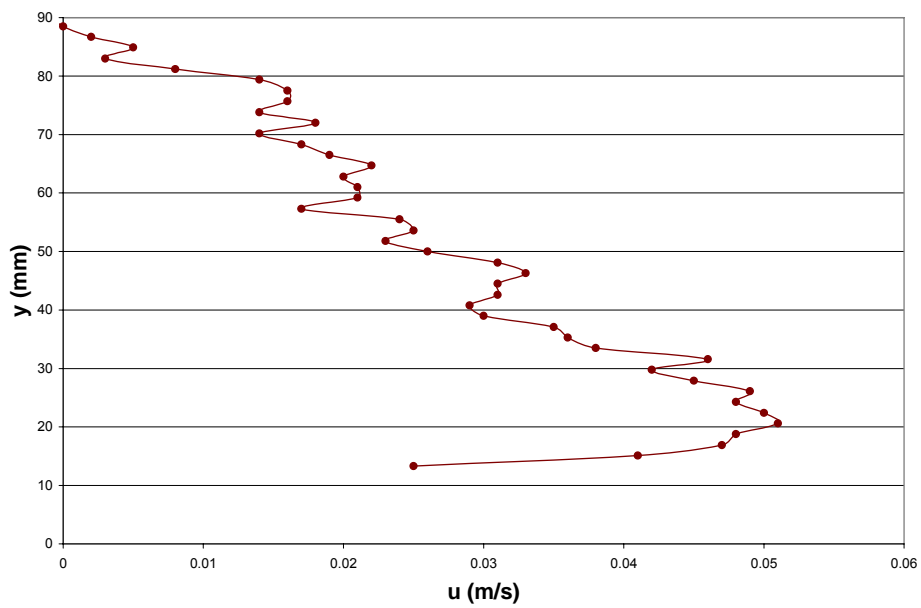


Figure B-3 The velocity profile at $x = 5a$ with a flow of $h \approx 35a$. Velocity vectors plotted with the measurement of PIV

APPENDIX C

DATA OF UPPER AND LOWER LIMITS OF SHIELDS DIAGRAM

Table C-1 Data of upper and lower limits in details.

Re*	Re	θ^*_{lower}	θ^*_{upper}	Fr²_{lower}	Fr²_{upper}
0.2	4.92	0.116	0.223	70.25	134.62
0.4	9.83	0.092	0.198	55.90	119.60
0.6	14.75	0.077	0.179	46.78	107.94
0.8	19.67	0.067	0.163	40.48	98.64
1	24.58	0.059	0.151	35.87	91.04
1.2	29.50	0.054	0.14	32.35	84.72
1.4	34.42	0.049	0.131	29.58	79.39
1.6	39.33	0.045	0.124	27.34	74.83
1.8	44.25	0.042	0.117	25.50	70.90
2	49.17	0.04	0.112	23.96	67.46
3	73.75	0.031	0.092	18.97	55.33
4	98.34	0.027	0.079	16.27	48.03
5	122.92	0.024	0.072	14.61	43.23
6	147.51	0.022	0.066	13.52	39.87
8	196.67	0.02	0.059	12.22	35.62
10	245.84	0.019	0.055	11.54	33.17
20	491.68	0.018	0.049	10.95	29.84
30	737.53	0.019	0.051	11.54	30.55
40	983.37	0.02	0.053	12.30	32.05
100	2458.42	0.026	0.066	15.75	39.93
150	3687.63	0.028	0.071	17.10	43.11
200	4916.84	0.029	0.074	17.73	44.59
300	7375.26	0.03	0.075	18.14	45.54
400	9833.68	0.03	0.076	18.21	45.67
500	12292.10	0.03	0.076	18.22	45.65
600	14750.52	0.03	0.075	18.21	45.61
700	17208.95	0.03	0.075	18.20	45.57
800	19667.37	0.03	0.075	18.19	45.54
900	22125.79	0.03	0.075	18.18	45.52

Table C-1 cont'd Data of upper and lower limits in details.

Re*	Re	θ^*_{lower}	θ^*_{upper}	Fr^2_{lower}	Fr^2_{upper}
1000	24584.21	0.03	0.075	18.18	45.50
2000	49168.42	0.03	0.075	18.15	45.41
3000	73752.62	0.03	0.075	18.15	45.39
4000	98336.83	0.03	0.075	18.14	45.37
5000	122921.04	0.03	0.075	18.14	45.36
6000	147505.25	0.03	0.075	18.14	45.36
7000	172089.46	0.03	0.075	18.14	45.35
8000	196673.66	0.03	0.075	18.14	45.35
9000	221257.87	0.03	0.075	18.14	45.35
10000	245842.08	0.03	0.075	18.14	45.35
20000	491684.16	0.03	0.075	18.13	45.34
30000	737526.24	0.03	0.075	18.13	45.33
40000	983368.32	0.03	0.075	18.13	45.33
50000	1229210.40	0.03	0.075	18.13	45.33
60000	1475052.48	0.03	0.075	18.13	45.33
70000	1720894.56	0.03	0.075	18.13	45.33
80000	1966736.64	0.03	0.075	18.13	45.33
90000	2212578.72	0.03	0.075	18.13	45.33
100000	2458420.80	0.03	0.075	18.13	45.33

APPENDIX D

A FURTHER RECOMMENDATION ON THE DESCRIPTION OF THE CUMULATIVE INTENSITY CONCEPT

As stated in Chapter 3, the observation of threshold of initiation of motion is very complicated to be described because it is very much observer – dependent. Only optical equipment can render the visual part of the experiment objective and can scatter the visual observation as quantitative measures. However, without the use of visual techniques, it is possible to describe the event with some parameters which are obtained by dimensional analysis. Shields (1936) and Yang (1973) studied on this and obtained their own plots both of which are well – known. In this part however, a relationship between the visual observations and an equation proposed by Melville and Coleman (2000), which is used for the calculation of critical shear velocity for the initiation motion, is studied. Equation D.1 was obtained by the explicit solution of the Shields' diagram.

$$\begin{aligned} u_{*c} &= 0.0115 + 0.0125 D_{50}^{1.4} & 0.1 \text{ mm} \leq D_{50} \leq 1 \text{ mm} \\ u_{*c} &= 0.0305 \sqrt{D_{50}} - \frac{0.0065}{D_{50}} & 1 \text{ mm} \leq D_{50} \leq 100 \text{ mm} \end{aligned} \quad (\text{D.1})$$

In Equation D.1, D_{50} is in mm, and u_{*c} is in m/s.

The cumulative intensity data versus the fifth root of the corresponding dimensionless velocity term, $(V_{ex}/u_*)^{(1/5)}$ are scattered and a best fit is

depicted on the data. The relationship fitted to the data in Figure D.1 is given in Equation D.2.

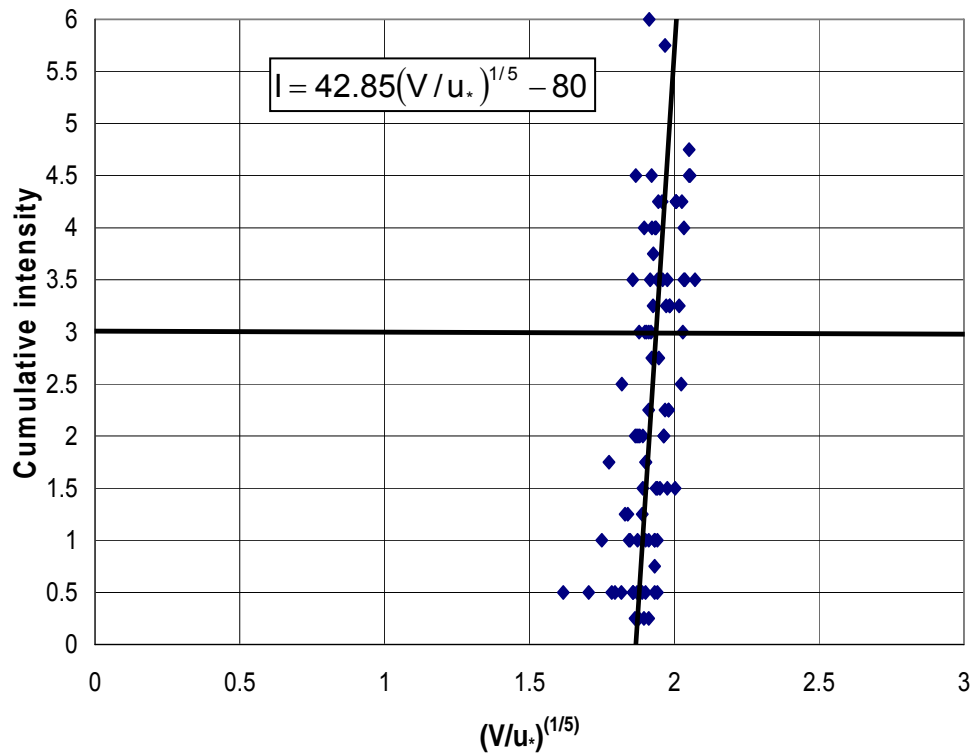


Figure D.1 The relationship between the cumulative intensity and the dimensionless velocity term.

$$I = 42.85(V/u_*)^{1/5} - 80 \quad (D.2)$$

In equation D.2, I is used to represent the cumulative intensity value.

Figure D.1 presents a preliminary study on the calibration of observations rather than the use of raw data decided by the observer

only. However, such as Shields' study, many data points are desired to define a band indicating the critical condition below which the motion is not started and above which the motion is assumed to be already started for a certain size of sediment particles. A further study on this definition will ensure the practical use of the basic aim of this study, which is to obtain a relation, likewise to Shields', to be used in reservoirs.